Density Model for Kogia Whales (*Kogia spp.*) for the U.S. East Coast: Supplementary Report

Duke University Marine Geospatial Ecology Lab*

Model Version 3.2 - 2015-10-07

Citation

When referencing our methodology or results generally, please cite our open-access article:

Roberts JJ, Best BD, Mannocci L, Fujioka E, Halpin PN, Palka DL, Garrison LP, Mullin KD, Cole TVN, Khan CB, McLellan WM, Pabst DA, Lockhart GG (2016) Habitat-based cetacean density models for the U.S. Atlantic and Gulf of Mexico. Scientific Reports 6: 22615. doi: 10.1038/srep22615

To reference this specific model or Supplementary Report, please cite:

Roberts JJ, Best BD, Mannocci L, Fujioka E, Halpin PN, Palka DL, Garrison LP, Mullin KD, Cole TVN, Khan CB, McLellan WM, Pabst DA, Lockhart GG (2015) Density Model for Kogia Whales (*Kogia spp.*) for the U.S. East Coast Version 3.2, 2015-10-07, and Supplementary Report. Marine Geospatial Ecology Lab, Duke University, Durham, North Carolina.

Copyright and License

Revision History

Version	Date	Description of changes
1	2014-10-15	Initial version.
2	2014-11-23	Reconfigured detection hierarchy and adjusted NARWSS detection functions based on additional information from Tim Cole. Updated documentation.
3	2015-03-06	Added a missing sighting from the Gulf of Mexico that affected the Oregon II detection function for both study areas. Refitted that detection function and the density model.
3.1	2015-05-14	Updated calculation of CVs. Switched density rasters to logarithmic breaks. No changes to the model.
3.2	2015-10-07	Updated the documentation. No changes to the model.

*For questions, or to offer feedback about this model or report, please contact Jason Roberts (jason.roberts@duke.edu)

Survey Data

Survey	Period	Length (1000 km)	Hours	Sightings
NEFSC Aerial Surveys	1995-2008	70	412	1
NEFSC NARWSS Harbor Porpoise Survey	1999-1999	6	36	0
NEFSC North Atlantic Right Whale Sighting Survey	1999-2013	432	2330	0
NEFSC Shipboard Surveys	1995-2004	16	1143	11
NJDEP Aerial Surveys	2008-2009	11	60	0
NJDEP Shipboard Surveys	2008-2009	14	836	0
SEFSC Atlantic Shipboard Surveys	1992-2005	28	1731	17
SEFSC Mid Atlantic Tursiops Aerial Surveys	1995-2005	35	196	0
SEFSC Southeast Cetacean Aerial Surveys	1992-1995	8	42	0
UNCW Cape Hatteras Navy Surveys	2011-2013	19	125	1
UNCW Early Marine Mammal Surveys	2002-2002	18	98	0
UNCW Jacksonville Navy Surveys	2009-2013	66	402	1
UNCW Onslow Navy Surveys	2007-2011	49	282	0
UNCW Right Whale Surveys	2005-2008	114	586	0
Virginia Aquarium Aerial Surveys	2012-2014	9	53	0
Total		895	8332	31

Table 2: Survey effort and sightings used in this model. Effort is tallied as the cumulative length of on-effort transects and hours the survey team was on effort. Sightings are the number of on-effort encounters of the modeled species for which a perpendicular sighting distance (PSD) was available. Off effort sightings and those without PSDs were omitted from the analysis.

Season	Months	Length (1000 km)	Hours	Sightings
All_Year	All	897	8332	31

Table 3: Survey effort and on-effort sightings having perpendicular sighting distances.

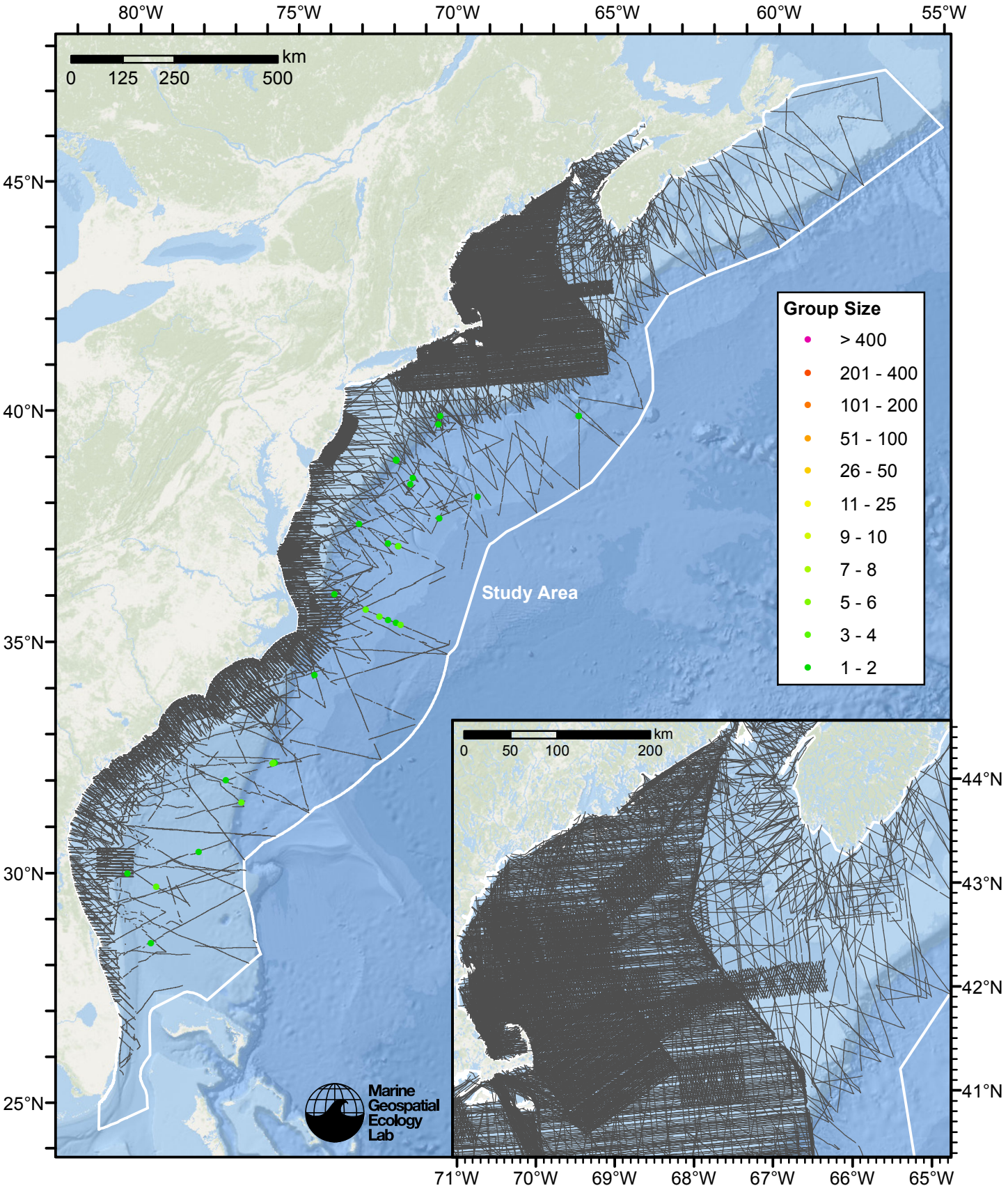

Figure 1: Kogia whales sightings and survey tracklines.

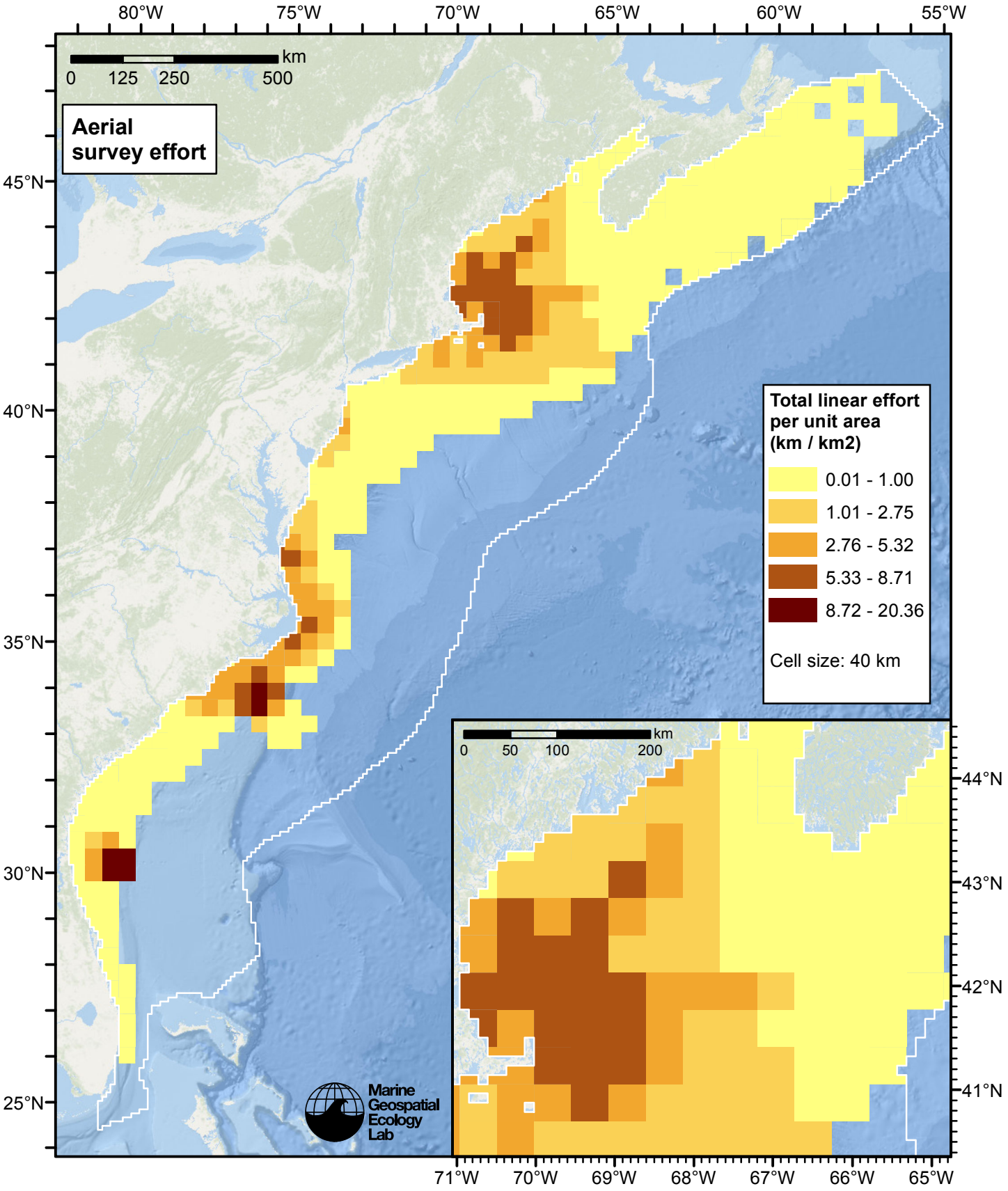

Figure 2: Aerial linear survey effort per unit area.

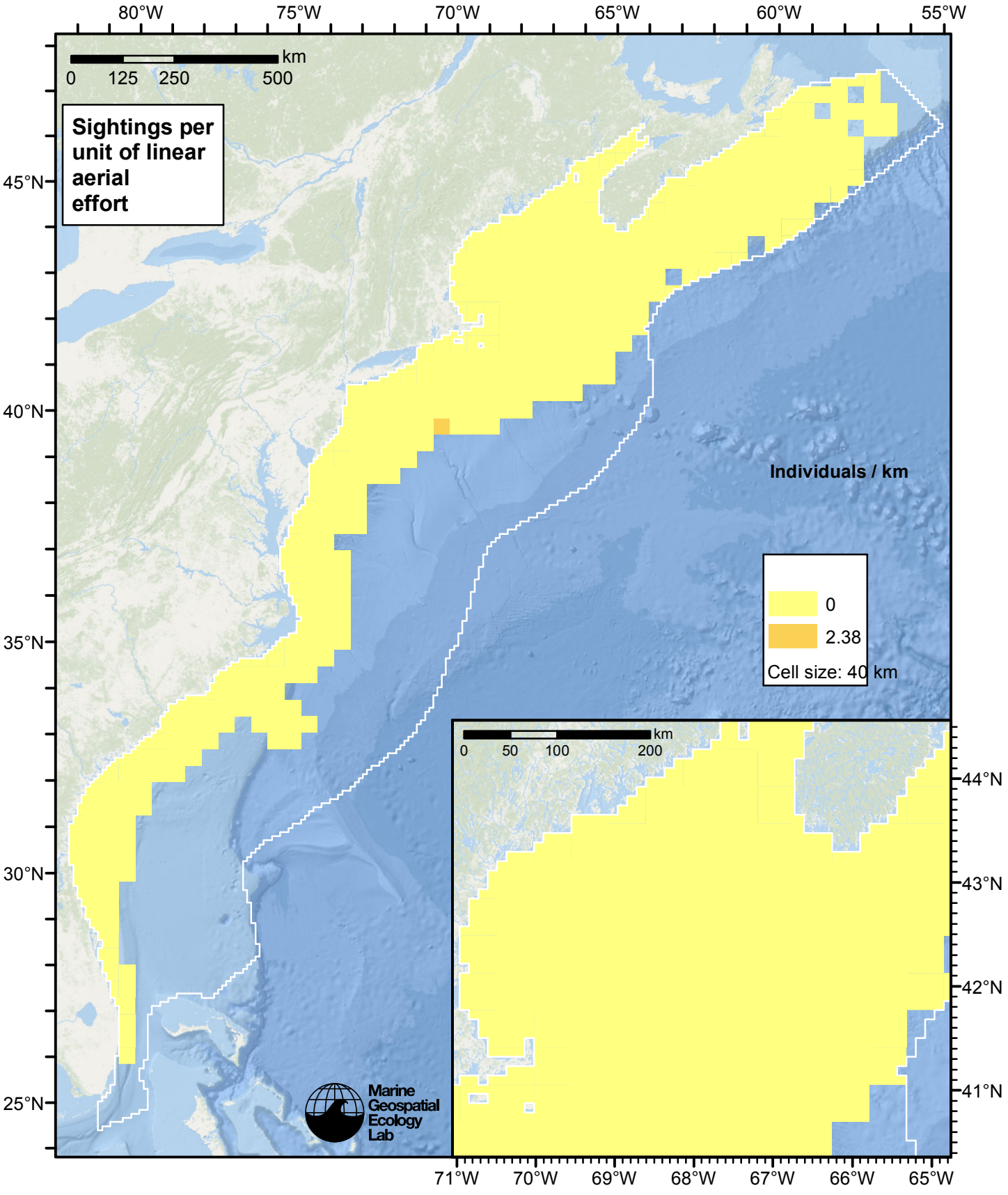

Figure 3: Kogia whales sightings per unit aerial linear survey effort.

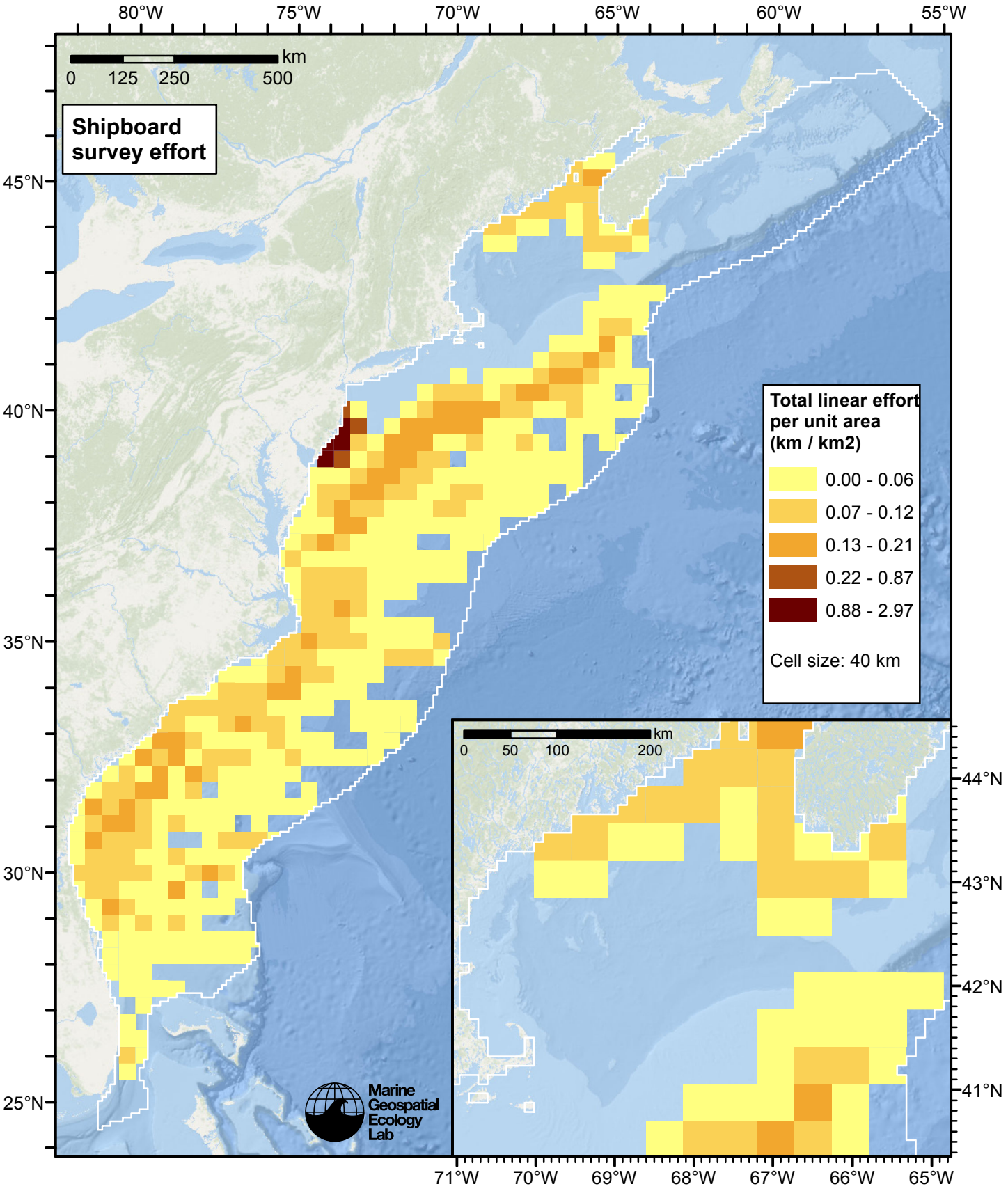

Figure 4: Shipboard linear survey effort per unit area.

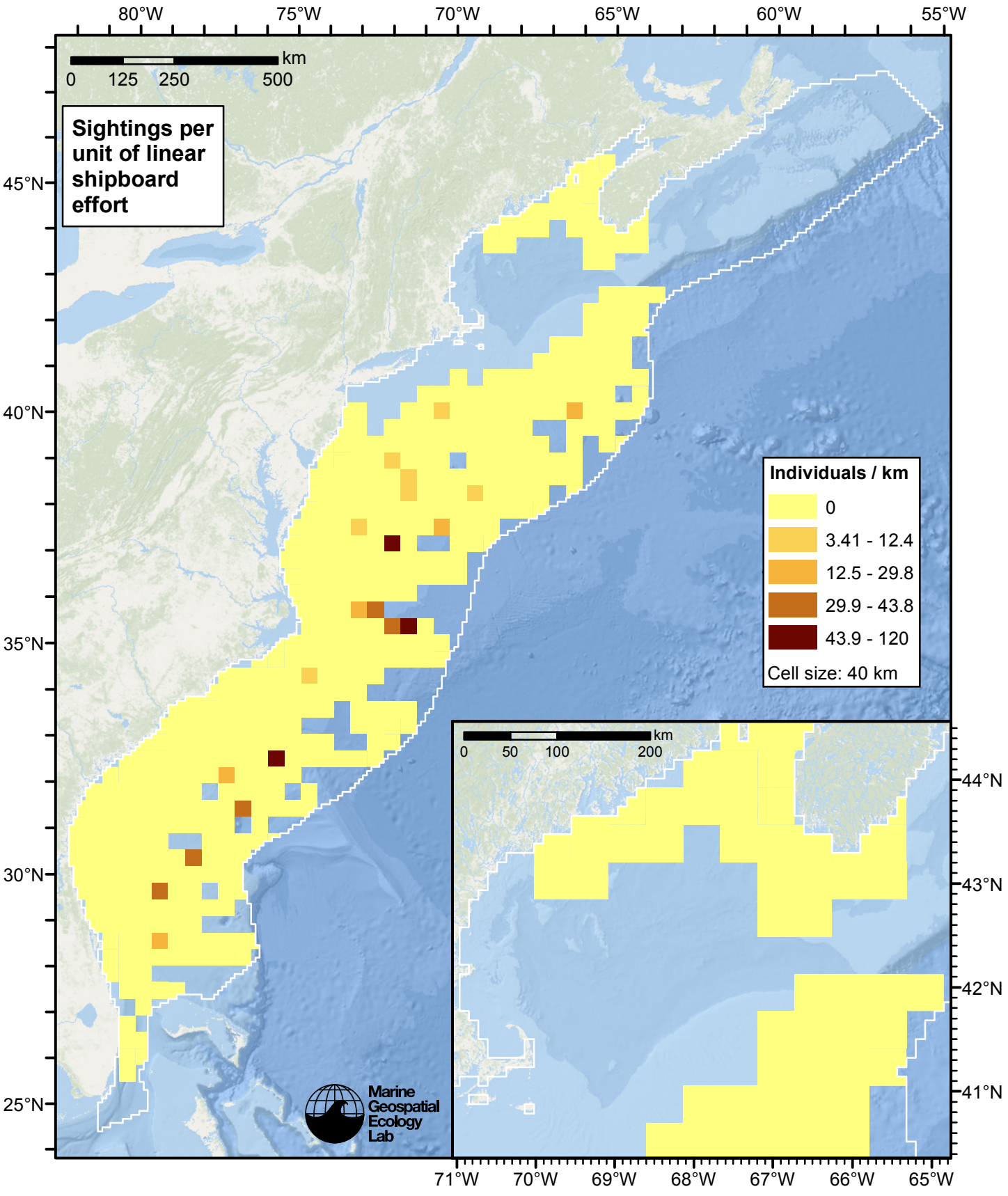

Figure 5: Kogia whales sightings per unit shipboard linear survey effort.

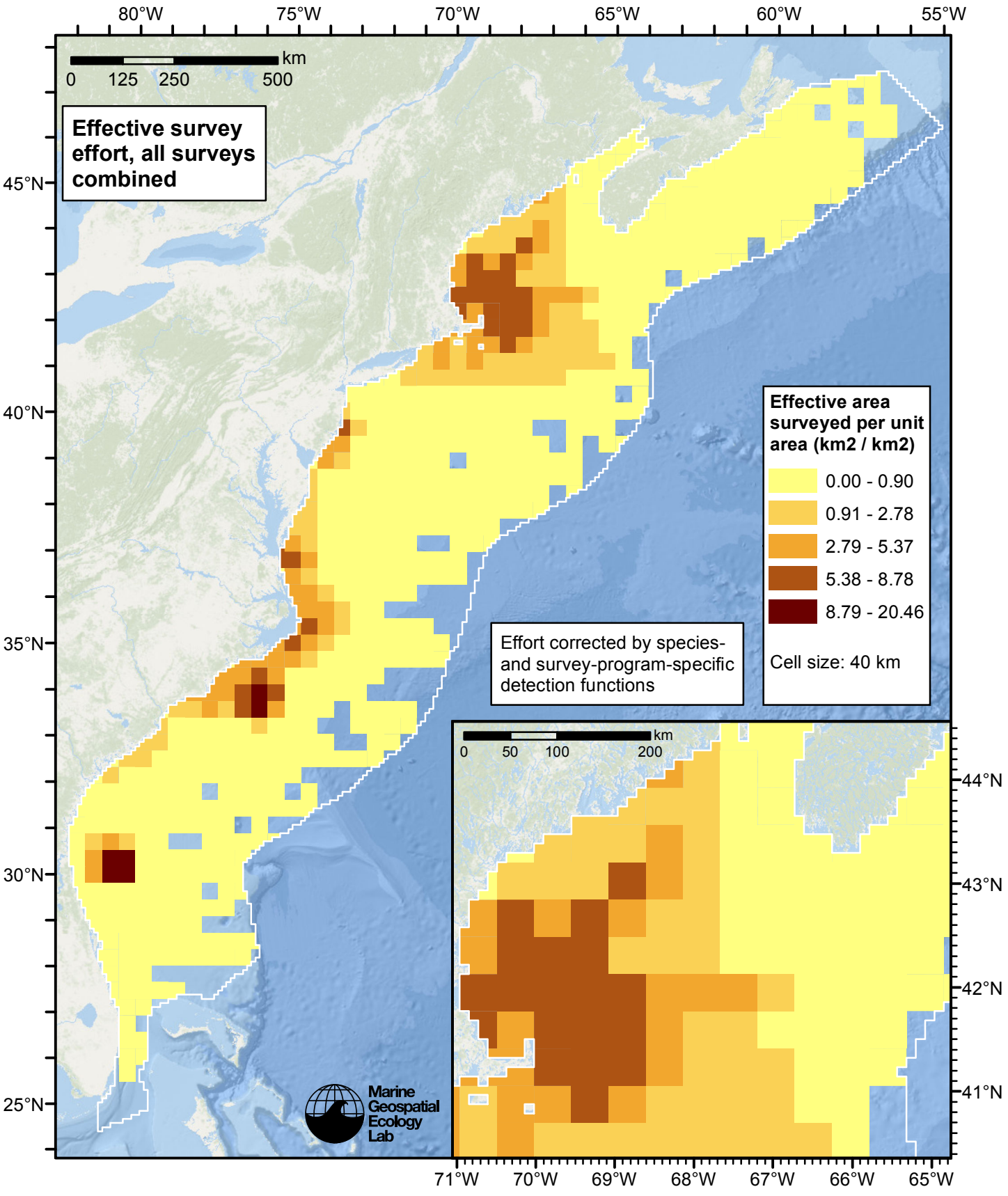

Figure 6: Effective survey effort per unit area, for all surveys combined. Here, effort is corrected by the species- and survey-program-specific detection functions used in fitting the density models.

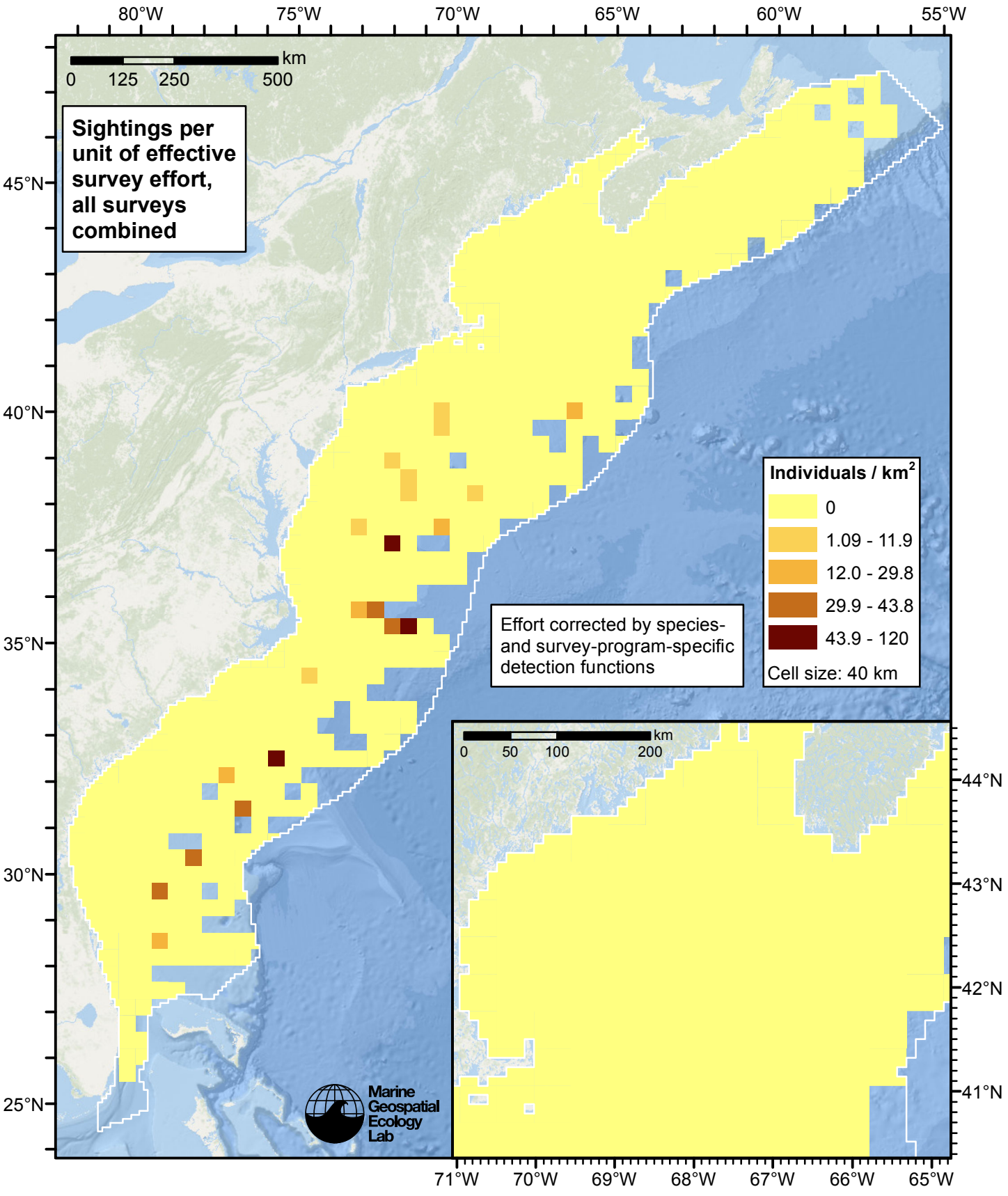

Figure 7: Kogia whales sightings per unit of effective survey effort, for all surveys combined. Here, effort is corrected by the species- and survey-program-specific detection functions used in fitting the density models.

Detection Functions

The detection hierarchy figures below show how sightings from multiple surveys were pooled to try to achieve Buckland et. al's (2001) recommendation that at least 60-80 sightings be used to fit a detection function. Leaf nodes, on the right, usually represent individual surveys, while the hierarchy to the left shows how they have been grouped according to how similar we believed the surveys were to each other in their detection performance.

At each node, the red or green number indicates the total number of sightings below that node in the hierarchy, and is colored green if 70 or more sightings were available, and red otherwise. If a grouping node has zero sightings–i.e. all of the surveys within it had zero sightings–it may be collapsed and shown as a leaf to save space.

Each histogram in the figure indicates a node where a detection function was fitted. The actual detection functions do not appear in this figure; they are presented in subsequent sections. The histogram shows the frequency of sightings by perpendicular sighting distance for all surveys contained by that node. Each survey (leaf node) recieves the detection function that is closest to it up the hierarchy. Thus, for common species, sufficient sightings may be available to fit detection functions deep in the hierarchy, with each function applying to only a few surveys, thereby allowing variability in detection performance between surveys to be addressed relatively finely. For rare species, so few sightings may be available that we have to pool many surveys together to try to meet Buckland's recommendation, and fit only a few coarse detection functions high in the hierarchy.

A blue Proxy Species tag indicates that so few sightings were available that, rather than ascend higher in the hierarchy to a point that we would pool grossly-incompatible surveys together, (e.g. shipboard surveys that used big-eye binoculars with those that used only naked eyes) we pooled sightings of similar species together instead. The list of species pooled is given in following sections.

Shipboard Surveys

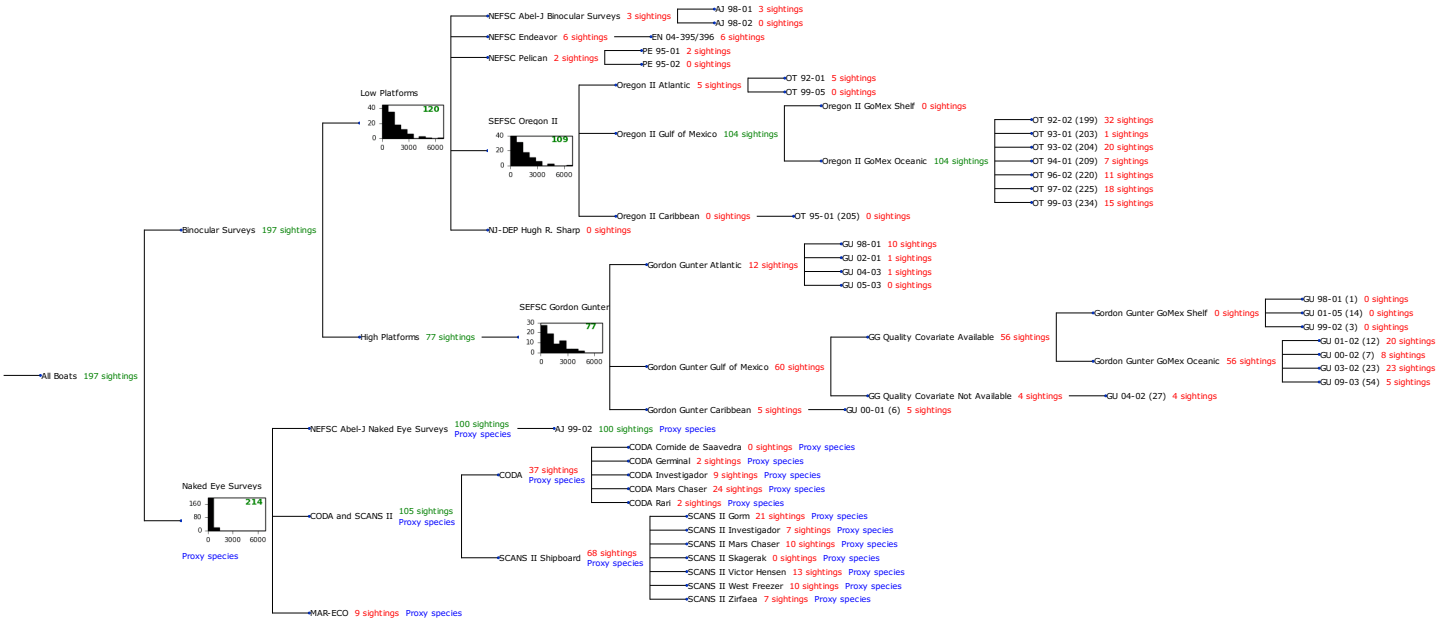

Figure 8: Detection hierarchy for shipboard surveys

Low Platforms

The sightings were right truncated at 6000m.

Covariate	Description
beaufort	Beaufort sea state.
size	Estimated size (number of individuals) of the sighted group.

Table 4: Covariates tested in candidate "multi-covariate distance sampling" (MCDS) detection functions.

Key	Adjustment	Order	Covariates	Succeeded	Δ AIC	Mean ESHW (m)
hn			beaufort, size	Yes	0.00	1986
hn			size	Yes	0.04	1980
hn	cos	2		Yes	2.43	1709
hr				Yes	3.41	1889
hr			size	Yes	4.31	1860
hr	poly	2		Yes	4.53	1825
hr	poly	4		Yes	4.55	1848
hr			beaufort	Yes	5.13	1900
hn				Yes	5.37	1973
hr			beaufort, size	Yes	5.63	1859
hn	cos	3		Yes	5.82	1737
hn			beaufort	Yes	7.09	1971
hn	herm	4		Yes	7.27	1971
hn	cos	1		No		

Table 5: Candidate detection functions for Low Platforms. The first one listed was selected for the density model.

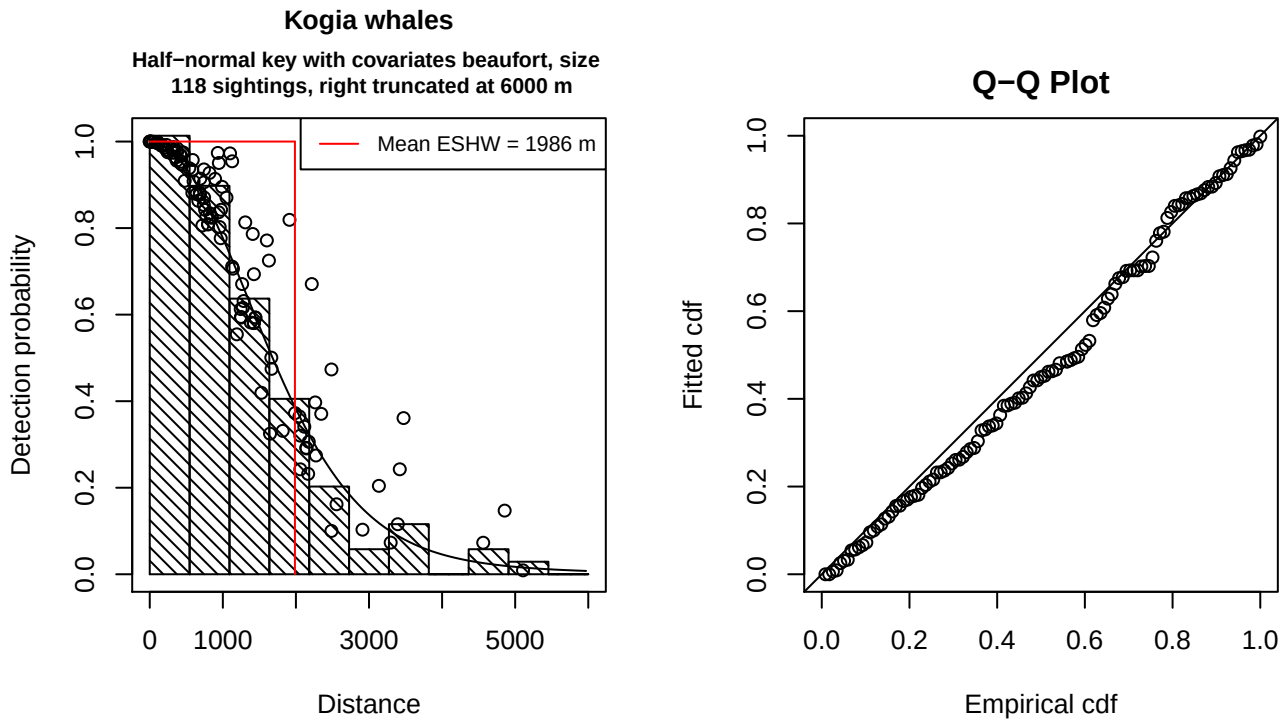

Figure 9: Detection function for Low Platforms that was selected for the density model

Statistical output for this detection function:

```
Summary for ds object
Number of observations :  118
Distance range         :  0  -  6000
AIC                    :  1904.963

Detection function:
 Half-normal key function

Detection function parameters
Scale Coefficients:
               estimate         se
(Intercept)  7.07472146 0.14440302
beaufort    -0.05459578 0.03816091
size         0.19900723 0.06641484

                      Estimate          SE         CV
Average p             0.3106064  0.02224362 0.07161352
N in covered region 379.9020253 40.10457611 0.10556558
```

Additional diagnostic plots:

Figure 10: Scatterplots showing the relationship between Beaufort sea state and perpendicular sighting distance, for all sightings (left) and only those not right truncated (right). The line is a simple linear regression.

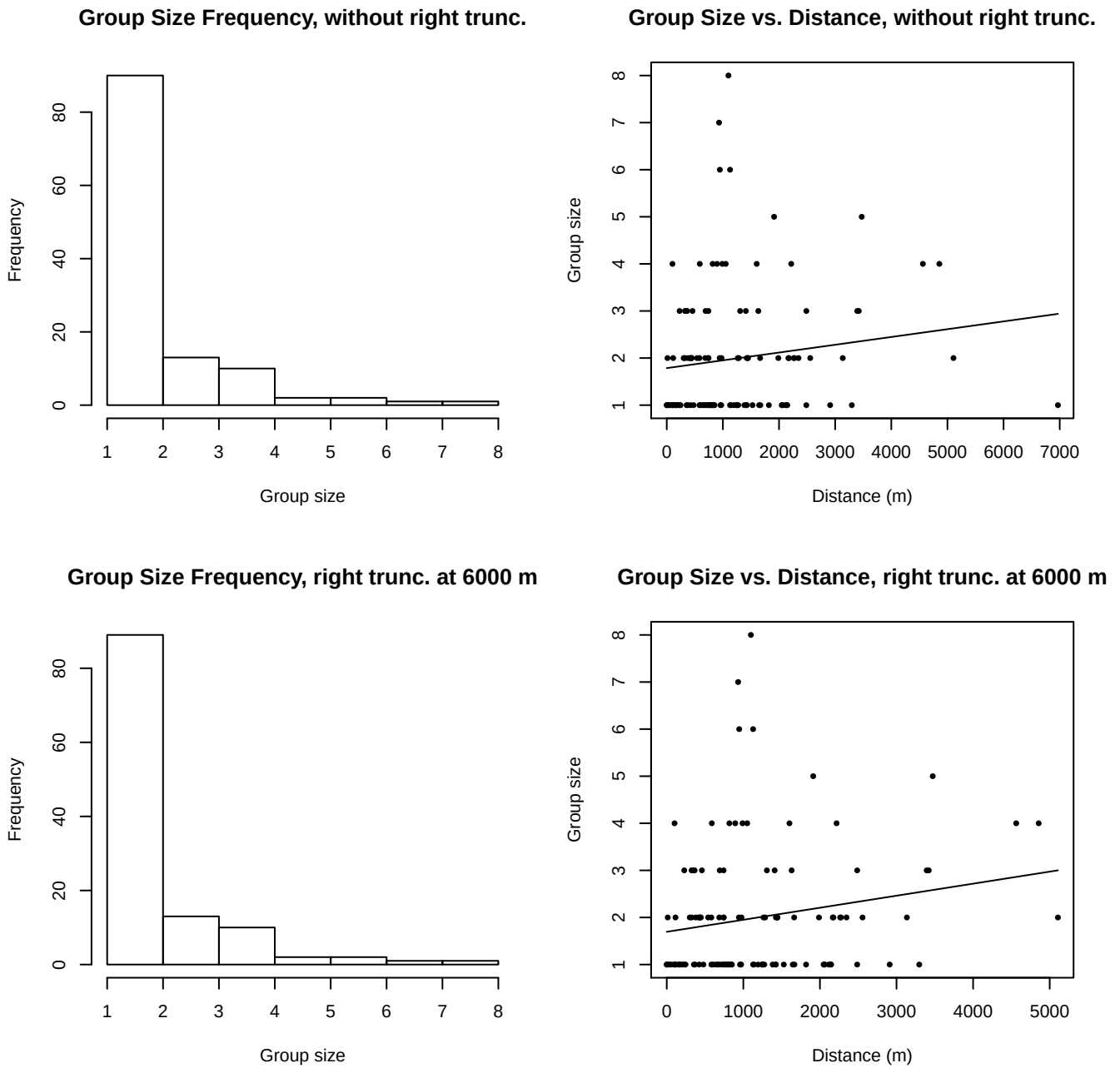

Figure 11: Histograms showing group size frequency and scatterplots showing the relationship between group size and perpendicular sighting distance, for all sightings (top row) and only those not right truncated (bottom row). In the scatterplot, the line is a simple linear regression.

SEFSC Oregon II

The sightings were right truncated at 6000m.

Covariate	Description
beaufort	Beaufort sea state.
quality	Survey-specific index of the quality of observation conditions, utilizing relevant factors other than Beaufort sea state (see methods).
size	Estimated size (number of individuals) of the sighted group.

Table 6: Covariates tested in candidate "multi-covariate distance sampling" (MCDS) detection functions.

Key	Adjustment	Order	Covariates	Succeeded	Δ AIC	Mean ESHW (m)
hn			quality, size	Yes	0.00	1934
hn			size	Yes	0.69	1947
hn			beaufort, quality, size	Yes	1.99	1935
hn			beaufort, size	Yes	2.11	1954
hr			quality	Yes	3.53	1962
hn			quality	Yes	4.35	1937
hr				Yes	4.38	1905
hn	cos	2		Yes	4.60	1714
hn				Yes	4.77	1936
hr			quality, size	Yes	4.88	1914
hr			beaufort, quality	Yes	5.53	1962
hr			size	Yes	5.86	1875
hr	poly	2		Yes	6.17	1875
hr	poly	4		Yes	6.32	1894
hr			beaufort	Yes	6.33	1909
hn	cos	3		Yes	6.46	1811
hr			beaufort, quality, size	Yes	6.86	1915
hr			beaufort, size	Yes	7.69	1874
hn	herm	4		No		
hn			beaufort	No		
hn			beaufort, quality	No		

Table 7: Candidate detection functions for SEFSC Oregon II. The first one listed was selected for the density model.

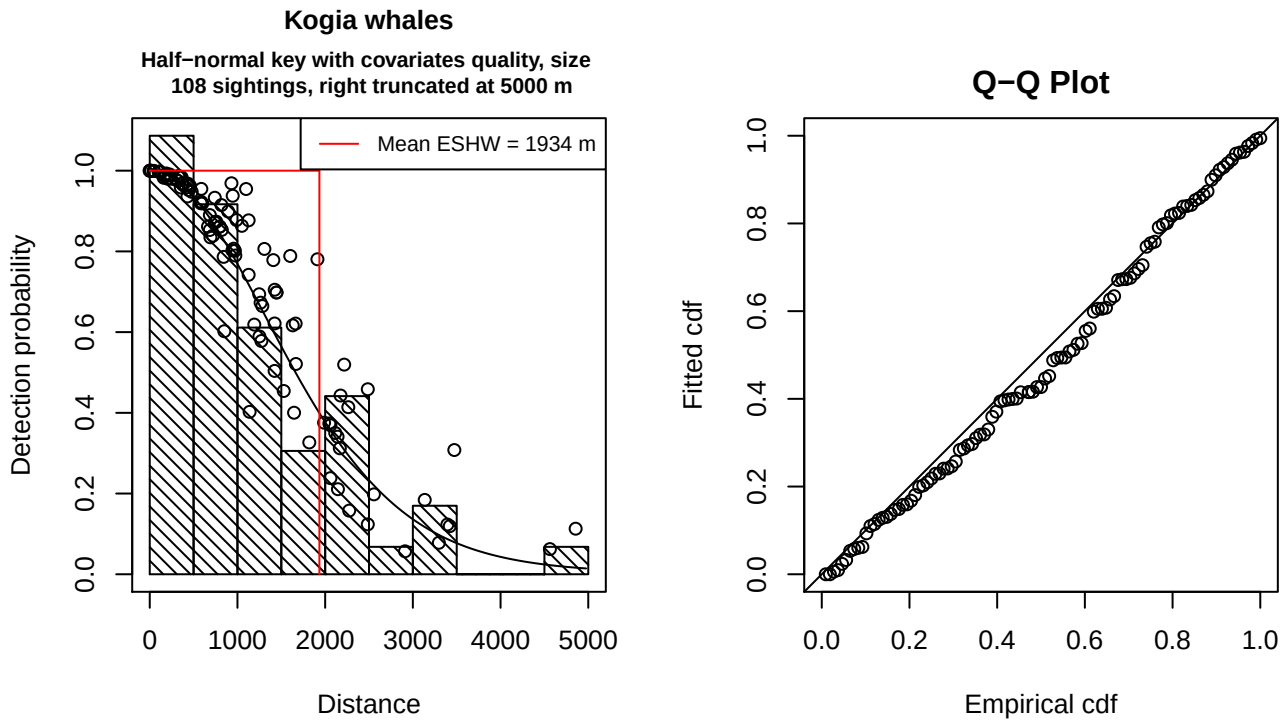

Figure 12: Detection function for SEFSC Oregon II that was selected for the density model

Statistical output for this detection function:

```
Summary for ds object
Number of observations :  108
Distance range         :  0  -  5000
AIC                    :  1738.51

Detection function:
 Half-normal key function

Detection function parameters
Scale Coefficients:
             estimate         se
(Intercept)  7.1308059 0.16525524
quality     -0.1095424 0.07073462
size         0.1551945 0.05746713

                      Estimate          SE         CV
Average p             0.3667174  0.02796449 0.07625624
N in covered region 294.5047099 32.08004956 0.10892882
```

Additional diagnostic plots:

Figure 13: Scatterplots showing the relationship between Beaufort sea state and perpendicular sighting distance, for all sightings (left) and only those not right truncated (right). The line is a simple linear regression.

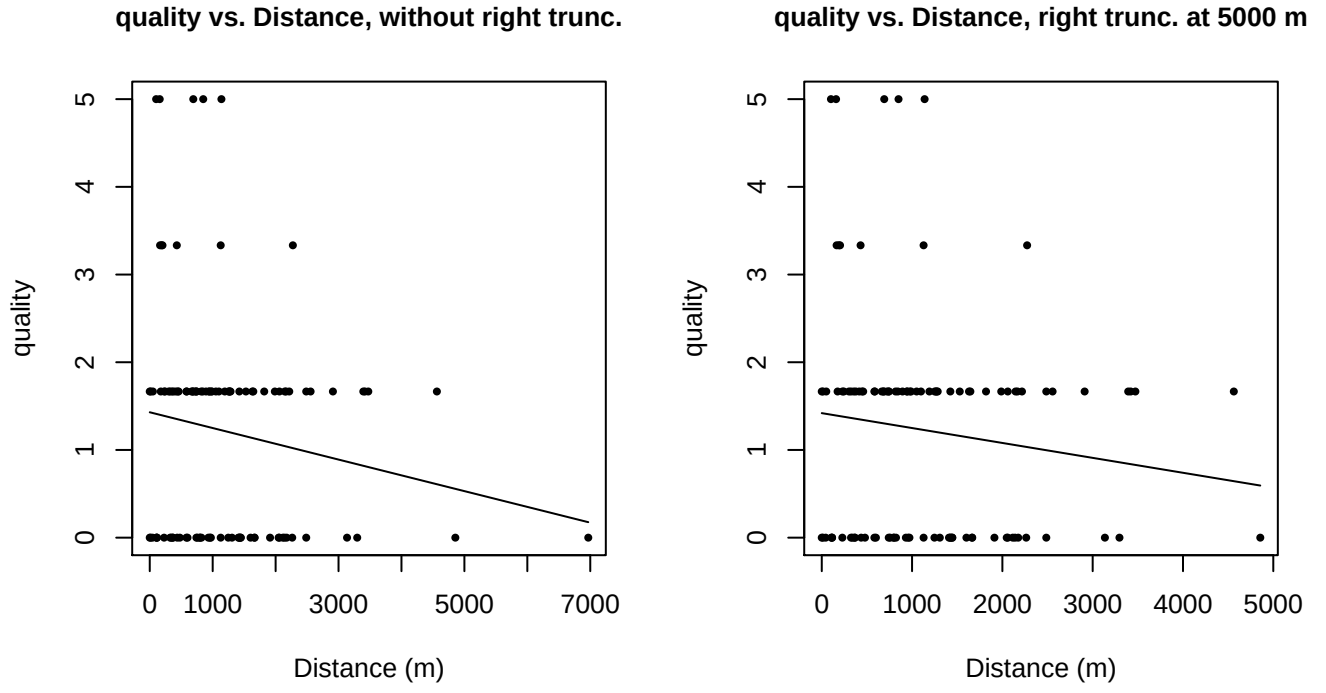

Figure 14: Scatterplots showing the relationship between the survey-specific index of the quality of observation conditions and perpendicular sighting distance, for all sightings (left) and only those not right truncated (right). Low values of the quality index correspond to better observation conditions. The line is a simple linear regression.

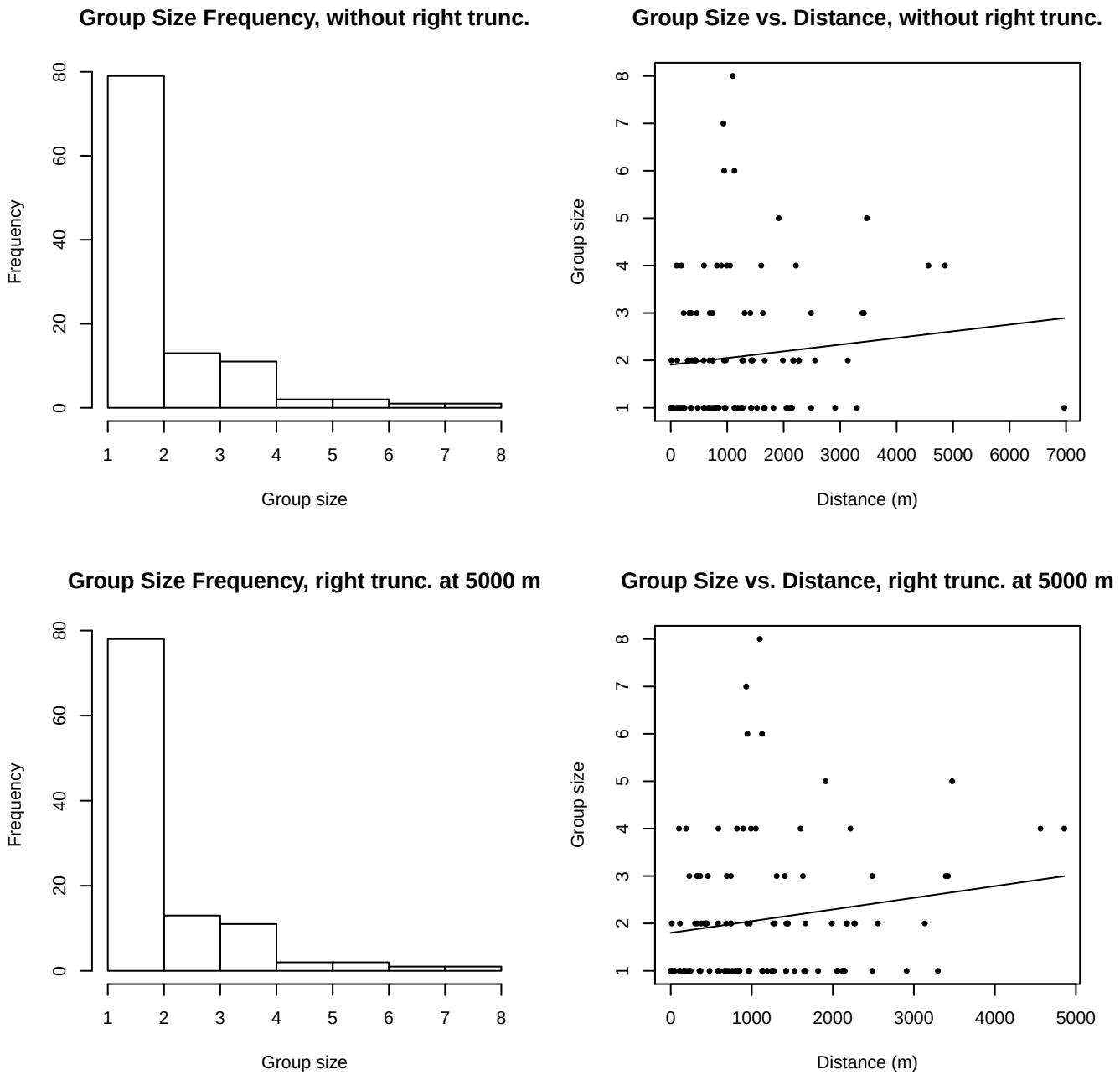

Figure 15: Histograms showing group size frequency and scatterplots showing the relationship between group size and perpendicular sighting distance, for all sightings (top row) and only those not right truncated (bottom row). In the scatterplot, the line is a simple linear regression.

SEFSC Gordon Gunter

The sightings were right truncated at 5000m.

Covariate	Description
beaufort	Beaufort sea state.
quality	Survey-specific index of the quality of observation conditions, utilizing relevant factors other than Beaufort sea state (see methods).
size	Estimated size (number of individuals) of the sighted group.

Table 8: Covariates tested in candidate "multi-covariate distance sampling" (MCDS) detection functions.

Key	Adjustment	Order	Covariates	Succeeded	Δ AIC	Mean ESHW (m)
hn			beaufort, size	Yes	0.00	2361
hn			beaufort, quality, size	Yes	0.85	2323
hr			beaufort, quality, size	Yes	0.89	2297
hr			beaufort, size	Yes	0.92	2312
hn			beaufort, quality	Yes	1.95	2353
hn			beaufort	Yes	4.31	2320
hr			beaufort, quality	Yes	5.06	2449
hn	cos	3		Yes	5.10	1866
hn				Yes	5.35	2332
hr			beaufort	Yes	6.14	2233
hn	cos	2		Yes	6.25	2074
hr			size	Yes	6.34	1976
hn			size	Yes	6.43	2328
hr	poly	4		Yes	6.76	1789
hn			quality	Yes	6.78	2332
hr				Yes	7.01	1894
hn	herm	4		Yes	7.31	2325
hr			quality, size	Yes	7.98	1966
hn			quality, size	Yes	8.35	2326
hr			quality	Yes	8.42	1870
hr	poly	2		Yes	9.01	1894
hn	cos	1		No		

Table 9: Candidate detection functions for SEFSC Gordon Gunter. The first one listed was selected for the density model.

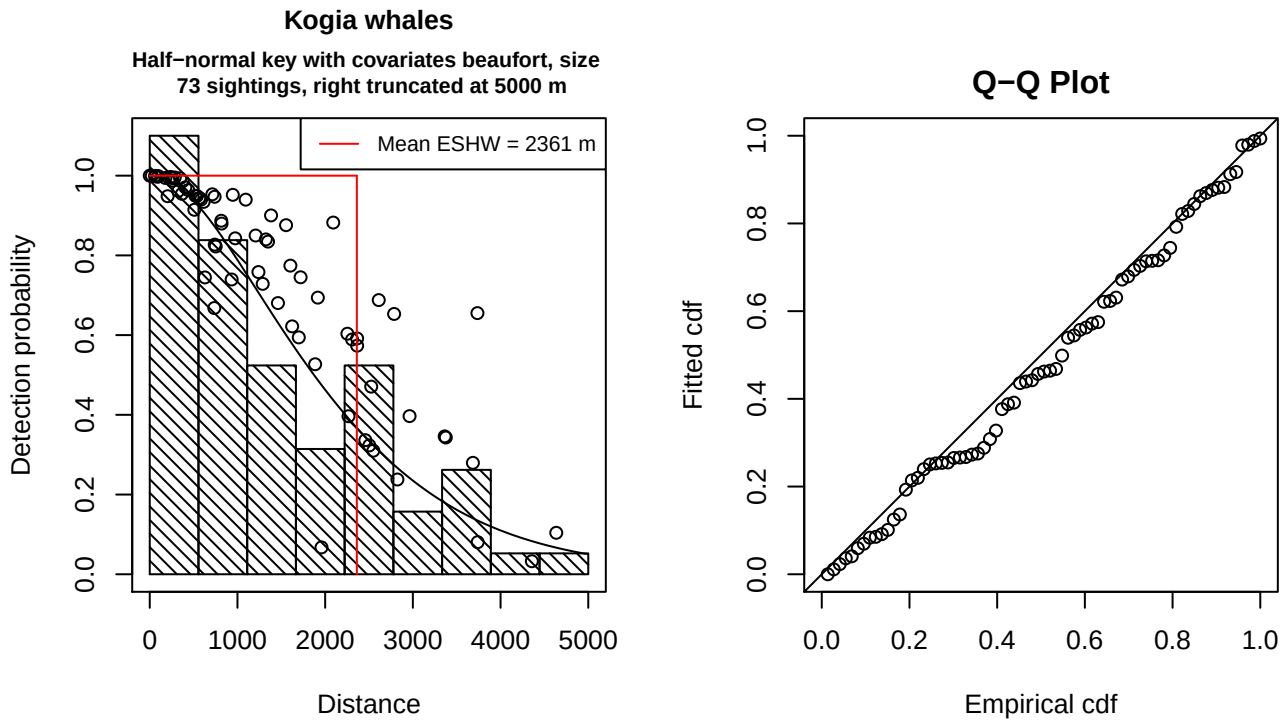

Figure 16: Detection function for SEFSC Gordon Gunter that was selected for the density model

Statistical output for this detection function:

```
Summary for ds object
Number of observations :  73
Distance range         :  0  -  5000
AIC                    :  1197.314

Detection function:
 Half-normal key function

Detection function parameters
Scale Coefficients:
             estimate        se
(Intercept)  7.4469239 0.1988146
beaufort    -0.3259967 0.0902056
size         0.2972217 0.1391281

                      Estimate          SE         CV
Average p             0.4249359  0.03836081 0.09027434
N in covered region 171.7905995 22.18392534 0.12913352
```

Additional diagnostic plots:

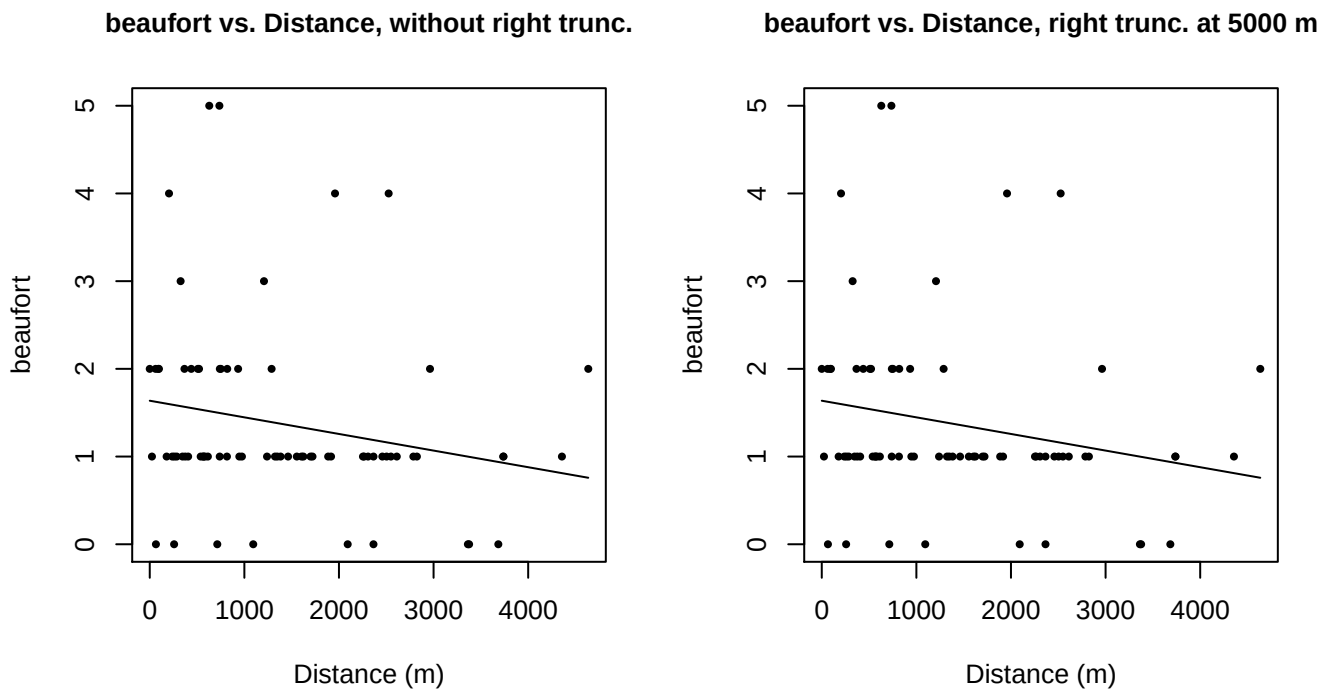

Figure 17: Scatterplots showing the relationship between Beaufort sea state and perpendicular sighting distance, for all sightings (left) and only those not right truncated (right). The line is a simple linear regression.

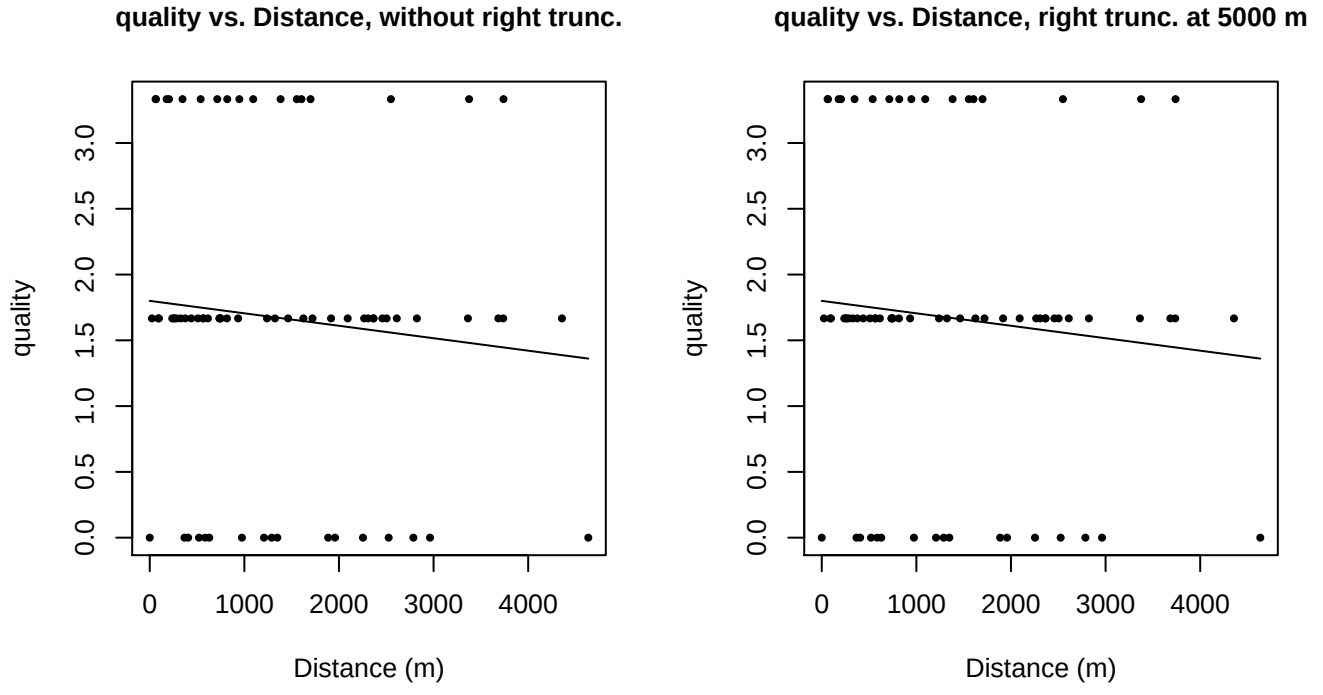

Figure 18: Scatterplots showing the relationship between the survey-specific index of the quality of observation conditions and perpendicular sighting distance, for all sightings (left) and only those not right truncated (right). Low values of the quality index correspond to better observation conditions. The line is a simple linear regression.

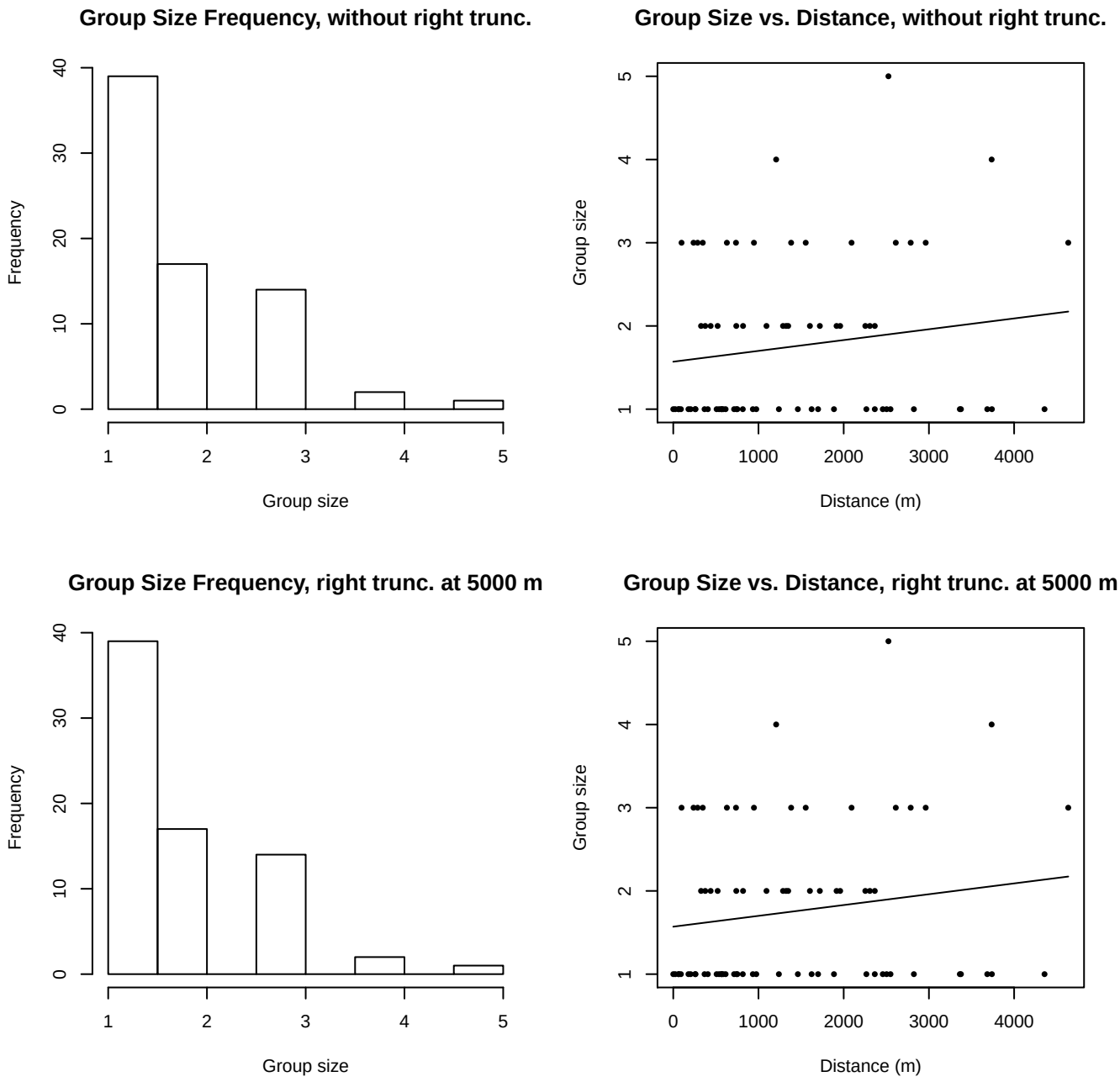

Figure 19: Histograms showing group size frequency and scatterplots showing the relationship between group size and perpendicular sighting distance, for all sightings (top row) and only those not right truncated (bottom row). In the scatterplot, the line is a simple linear regression.

Naked Eye Surveys

Because this taxon was sighted too infrequently to fit a detection function to its sightings alone, we fit a detection function to the pooled sightings of several other species that we believed would exhibit similar detectability. These "proxy species" are listed below.

Reported By Observer	Common Name	n
Balaenoptera acutorostrata	Minke whale	177
Kogia	Pygmy or dwarf sperm whale	0

Kogia breviceps	Pygmy sperm whale	0
Kogia sima	Dwarf sperm whale	0
Mesoplodon	Beaked whale	21
Mesoplodon bidens	Sowerby's beaked whale	5
Mesoplodon densirostris	Blainville's beaked whale	0
Mesoplodon europaeus	Gervais' beaked whale	0
Mesoplodon mirus	True's beaked whale	0
Ziphiidae	Unidentified beaked whale	1
Ziphius cavirostris	Cuvier's beaked whale	10
Total		214

Table 10: Proxy species used to fit detection functions for Naked Eye Surveys. The number of sightings, n, is before truncation.

The sightings were right truncated at 1000m.

Covariate	Description
beaufort	Beaufort sea state.
size	Estimated size (number of individuals) of the sighted group.

Table 11: Covariates tested in candidate "multi-covariate distance sampling" (MCDS) detection functions.

Key	Adjustment	Order	Covariates	Succeeded	Δ AIC	Mean ESHW (m)
hn	cos	3		Yes	0.00	352
hr	poly	4		Yes	0.70	372
hn	cos	2		Yes	0.84	376
hr	poly	2		Yes	1.22	354
hr			beaufort	Yes	2.84	393
hr				Yes	3.25	388
hn				Yes	4.70	440
hn			beaufort	Yes	5.40	441
hn	herm	4		Yes	6.57	439
hn			size	Yes	6.64	440
hn			beaufort, size	Yes	7.29	441
hn	cos	1		No		
hr			size	No		
hr			beaufort, size	No		

Table 12: Candidate detection functions for Naked Eye Surveys. The first one listed was selected for the density model.

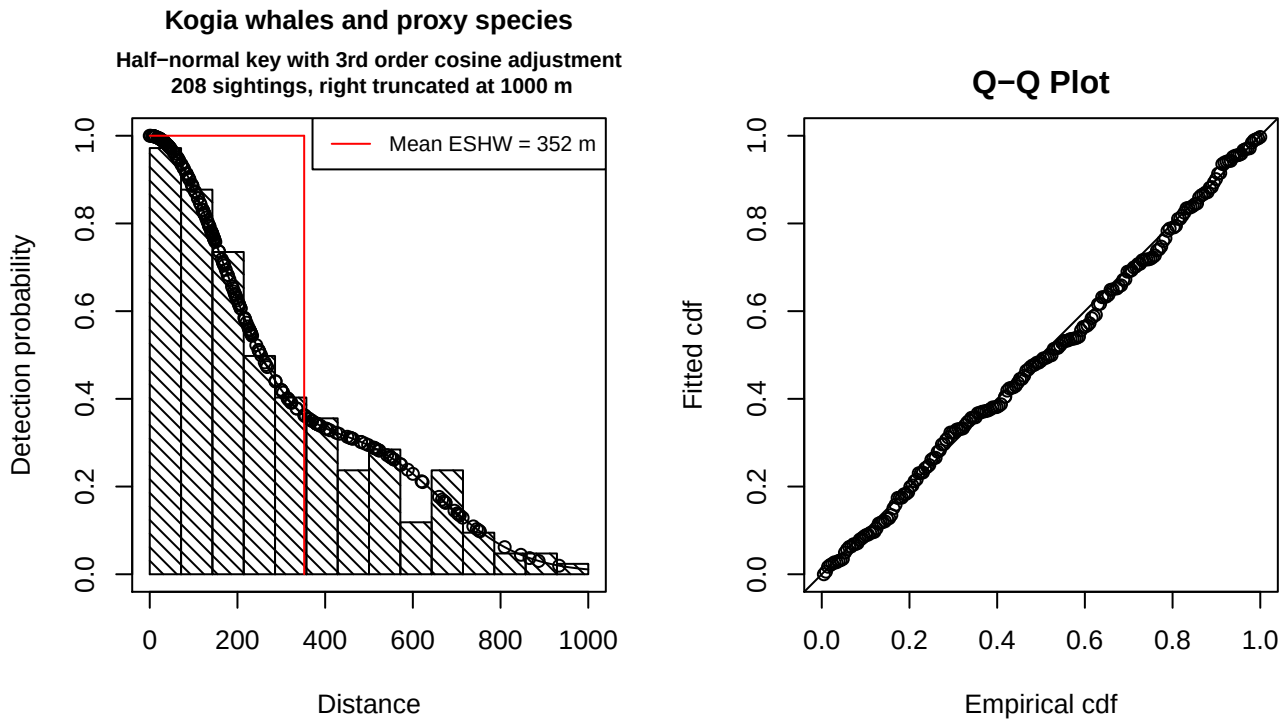

Figure 20: Detection function for Naked Eye Surveys that was selected for the density model

Statistical output for this detection function:

```
Summary for ds object
Number of observations :  208
Distance range         :  0  -  1000
AIC                    :  2729.029

Detection function:
 Half-normal key function with cosine adjustment term of order 3

Detection function parameters
Scale Coefficients:
            estimate         se
(Intercept) 5.870087 0.05063589

Adjustment term parameter(s):
              estimate         se
cos, order 3 0.2567371 0.09720518


Monotonicity constraints were enforced.
                       Estimate          SE         CV
Average p             0.3521876  0.03153628 0.08954398
N in covered region 590.5943580 62.31430343 0.10551117

Monotonicity constraints were enforced.
```

Additional diagnostic plots:

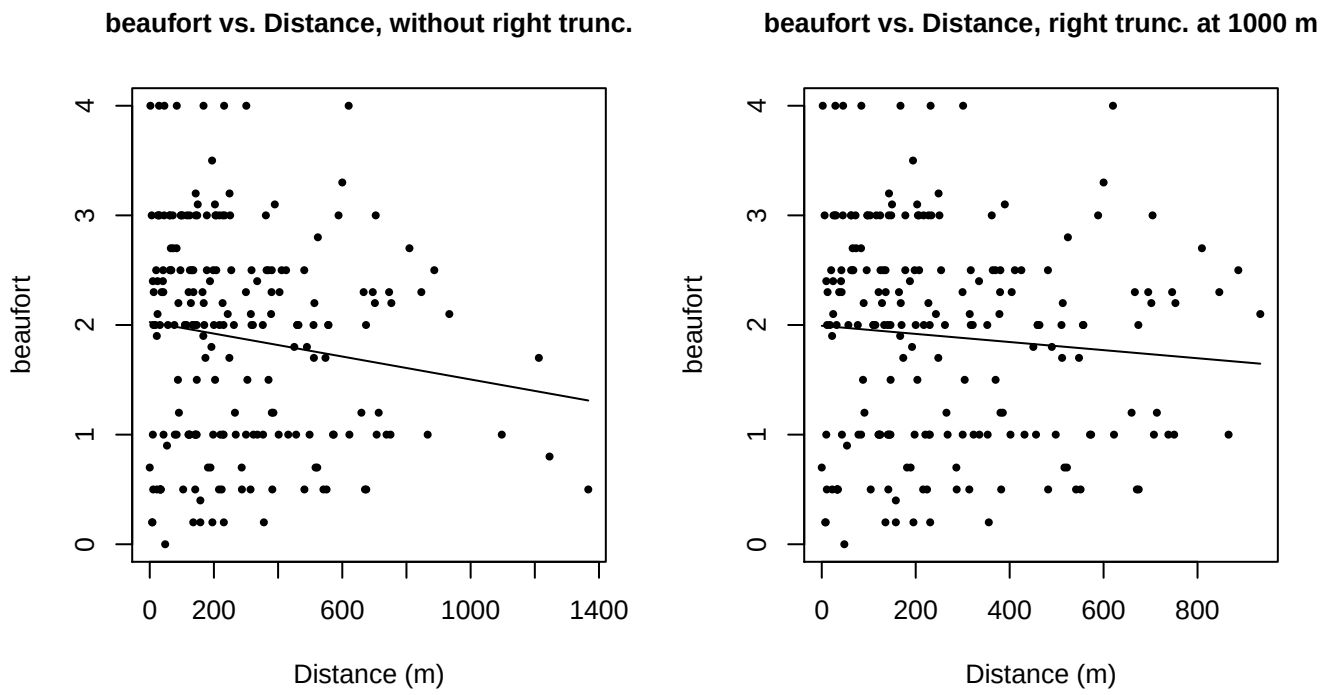

Figure 21: Scatterplots showing the relationship between Beaufort sea state and perpendicular sighting distance, for all sightings (left) and only those not right truncated (right). The line is a simple linear regression.

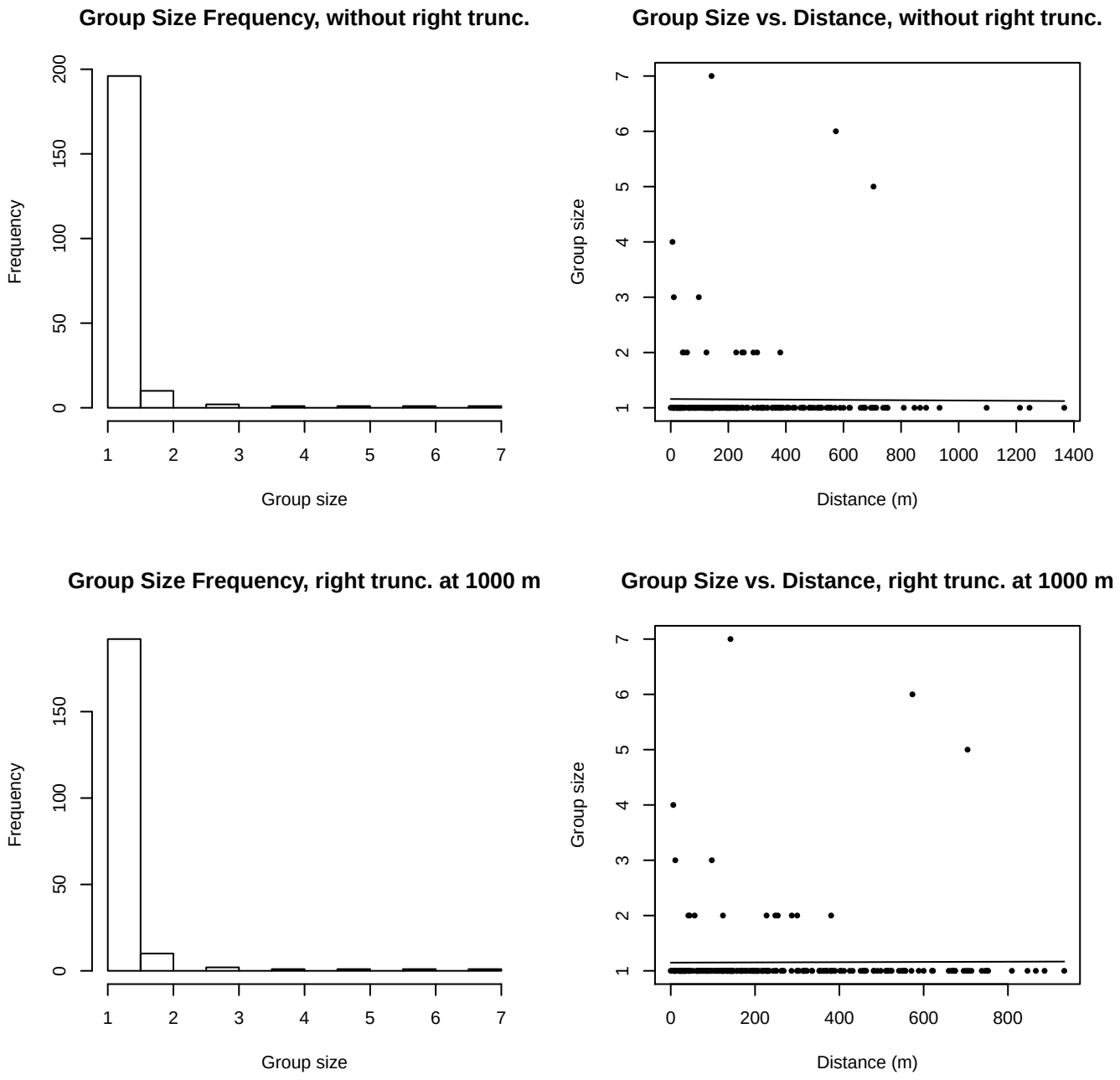

Figure 22: Histograms showing group size frequency and scatterplots showing the relationship between group size and perpendicular sighting distance, for all sightings (top row) and only those not right truncated (bottom row). In the scatterplot, the line is a simple linear regression.

Aerial Surveys

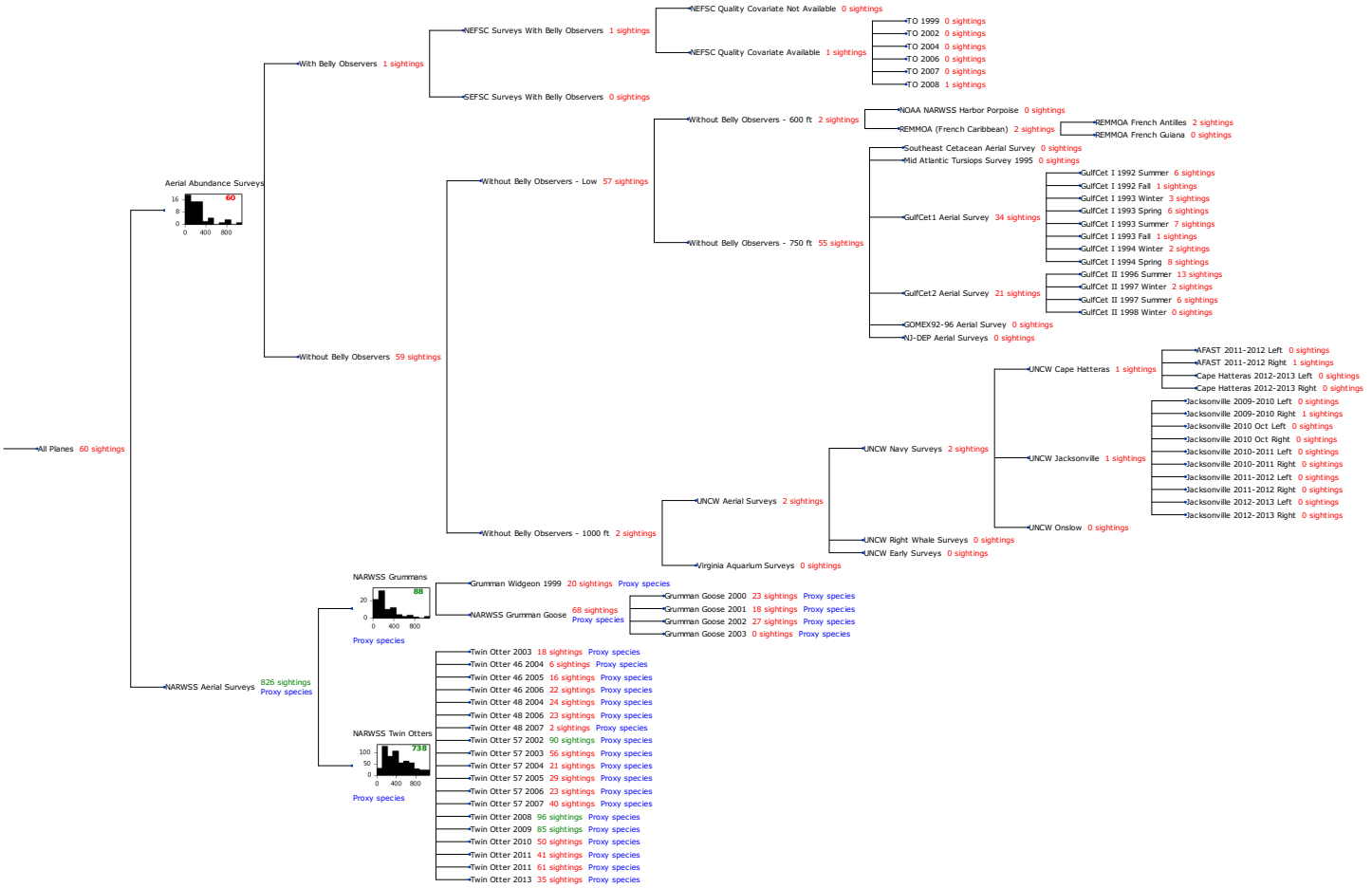

Figure 23: Detection hierarchy for aerial surveys

Aerial Abundance Surveys

The sightings were right truncated at 628m. Due to a reduced frequency of sightings close to the trackline that plausibly resulted from the behavior of the observers and/or the configuration of the survey platform, the sightings were left truncted as well. Sightings closer than 83 m to the trackline were omitted from the analysis, and it was assumed that the the area closer to the trackline than this was not surveyed. This distance was estimated by inspecting histograms of perpendicular sighting distances. The vertical sighting angles were heaped at 10 degree increments, so the candidate detection functions were fitted using linear bins scaled accordingly.

Key	Adjustment	Order	Covariates	Succeeded	Δ AIC	Mean ESHW (m)
hn				Yes	0.00	193
hn	cos	3		Yes	1.75	148
hn	herm	4		Yes	1.92	204
hn	cos	2		Yes	1.98	202
hr				Yes	2.63	263
hr	poly	2		Yes	4.24	183
hr	poly	4		Yes	4.51	216

Table 13: Candidate detection functions for Aerial Abundance Surveys. The first one listed was selected for the density model.

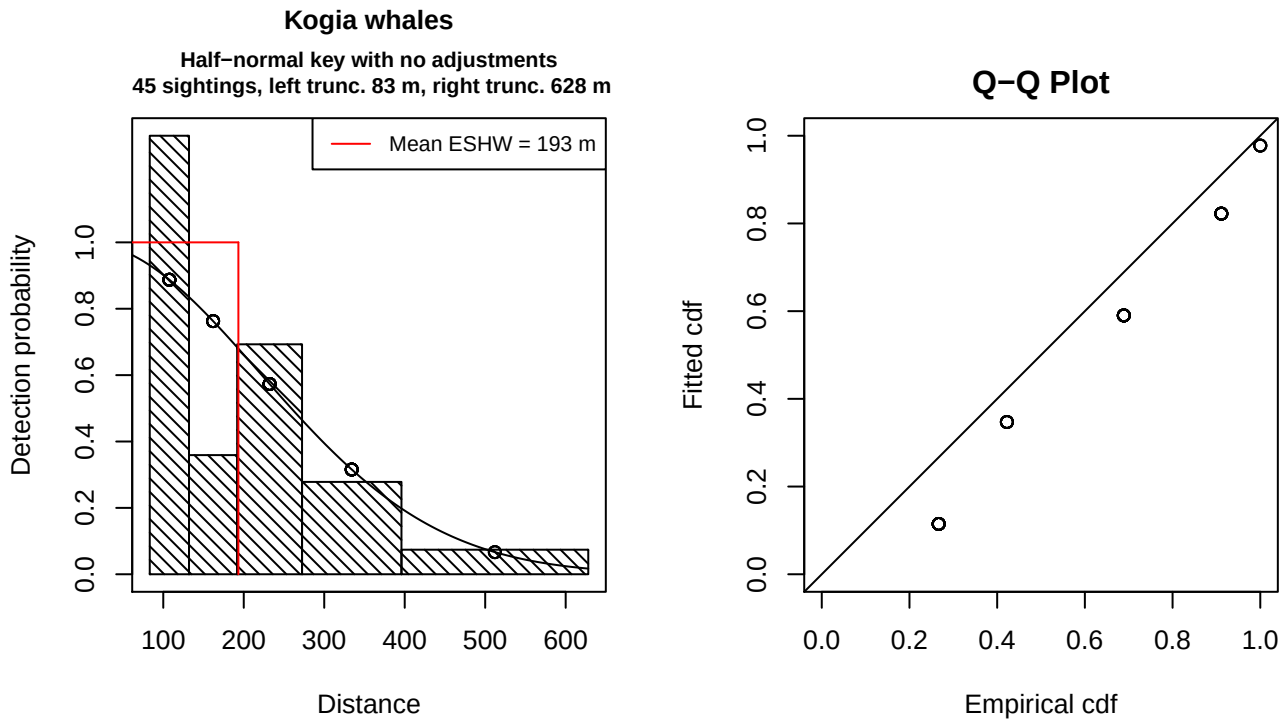

Figure 24: Detection function for Aerial Abundance Surveys that was selected for the density model

Statistical output for this detection function:

```
Summary for ds object
Number of observations :  45
Distance range         :  83.2036  -  628.0733
AIC                    :  142.9171

Detection function:
 Half-normal key function

Detection function parameters
Scale Coefficients:
            estimate       se
(Intercept) 5.393895 0.118983

                       Estimate          SE        CV
Average p             0.3078457  0.04927828 0.1600746
N in covered region 146.1771392 29.60045282 0.2024971
```

Additional diagnostic plots:

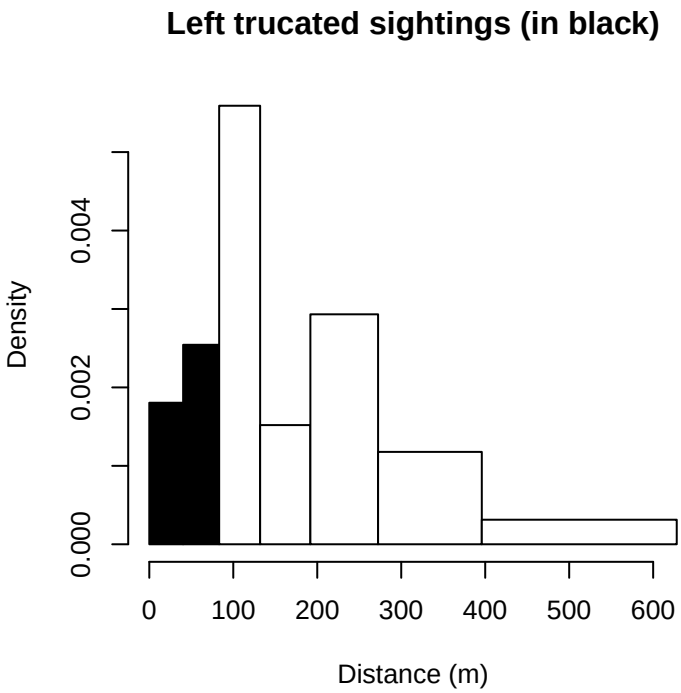

Figure 25: Density of sightings by perpendicular distance for Aerial Abundance Surveys. Black bars on the left show sightings that were left truncated.

NARWSS Grummans

Because this taxon was sighted too infrequently to fit a detection function to its sightings alone, we fit a detection function to the pooled sightings of several other species that we believed would exhibit similar detectability. These "proxy species" are listed below.

Reported By Observer	Common Name	n
Balaenoptera acutorostrata	Minke whale	88
Kogia	Pygmy or dwarf sperm whale	0
Kogia breviceps	Pygmy sperm whale	0
Kogia sima	Dwarf sperm whale	0
Mesoplodon	Beaked whale	0
Mesoplodon bidens	Sowerby's beaked whale	0
Mesoplodon densirostris	Blainville's beaked whale	0
Mesoplodon europaeus	Gervais' beaked whale	0
Mesoplodon mirus	True's beaked whale	0
Ziphiidae	Unidentified beaked whale	0
Ziphius cavirostris	Cuvier's beaked whale	0
Total		88

Table 14: Proxy species used to fit detection functions for NARWSS Grummans. The number of sightings, n, is before truncation.

The sightings were right truncated at 1500m.

Covariate	Description
beaufort	Beaufort sea state.
quality	Survey-specific index of the quality of observation conditions, utilizing relevant factors other than Beaufort sea state (see methods).
size	Estimated size (number of individuals) of the sighted group.

Table 15: Covariates tested in candidate "multi-covariate distance sampling" (MCDS) detection functions.

Key	Adjustment	Order	Covariates	Succeeded	Δ AIC	Mean ESHW (m)
hr			quality	Yes	0.00	450
hr			beaufort, quality	Yes	0.42	448
hr			beaufort	Yes	11.67	397
hr				Yes	11.73	388
hn	cos	2		Yes	12.57	383
hn			quality	Yes	12.59	441
hr	poly	4		Yes	12.95	386
hr	poly	2		Yes	13.20	384
hn	cos	3		Yes	16.21	366
hn				Yes	18.08	451
hn	herm	4		Yes	20.01	451
hn	cos	1		No		
hn			beaufort	No		
hr			size	No		
hn			size	No		
hn			beaufort, quality	No		
hr			beaufort, size	No		
hn			beaufort, size	No		
hr			quality, size	No		
hn			quality, size	No		
hr			beaufort, quality, size	No		
hn			beaufort, quality, size	No		

Table 16: Candidate detection functions for NARWSS Grummans. The first one listed was selected for the density model.

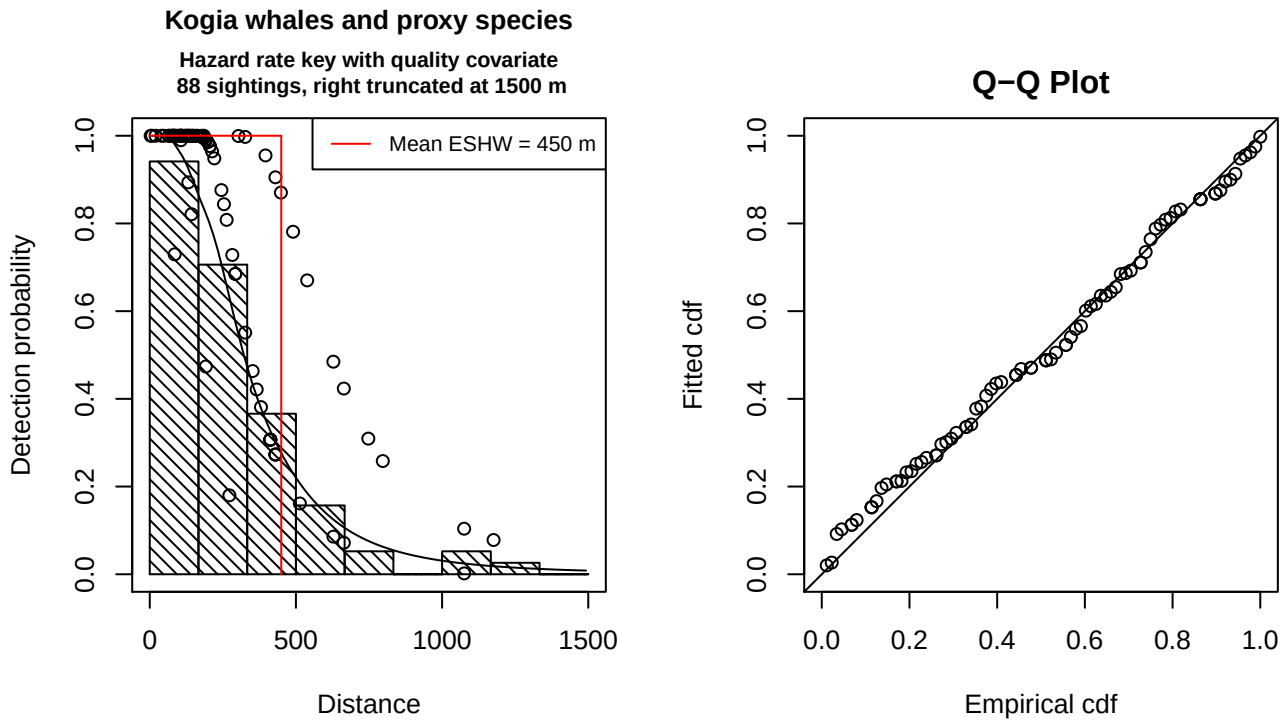

Figure 26: Detection function for NARWSS Grummans that was selected for the density model

Statistical output for this detection function:

```
Summary for ds object
Number of observations :  88
Distance range         :  0  -  1500
AIC                    :  1147.652

Detection function:
 Hazard-rate key function

Detection function parameters
Scale Coefficients:
             estimate        se
(Intercept)  6.3199108 0.1582062
quality     -0.4783316 0.1116862

Shape parameters:
            estimate        se
(Intercept) 1.207417 0.1695945

                       Estimate          SE        CV
Average p             0.2556843  0.02922365 0.1142958
N in covered region 344.1744315 51.07685302 0.1484040
```

Additional diagnostic plots:

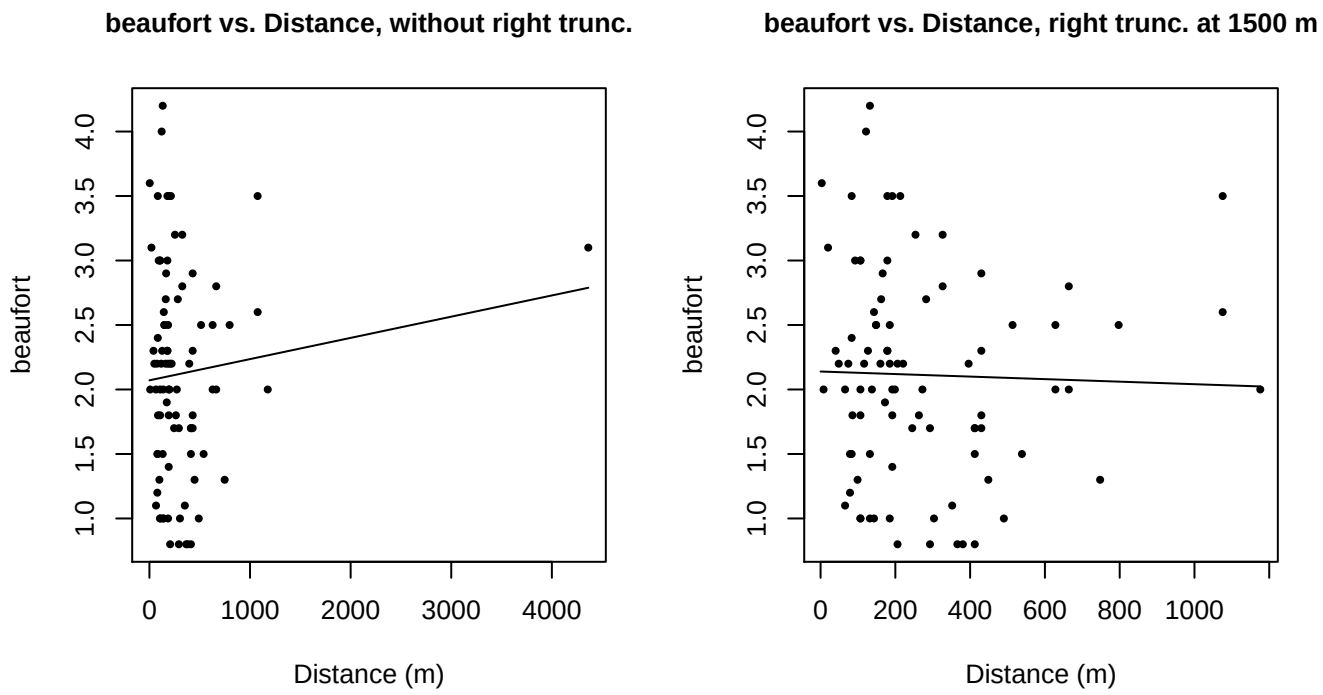

Figure 27: Scatterplots showing the relationship between Beaufort sea state and perpendicular sighting distance, for all sightings (left) and only those not right truncated (right). The line is a simple linear regression.

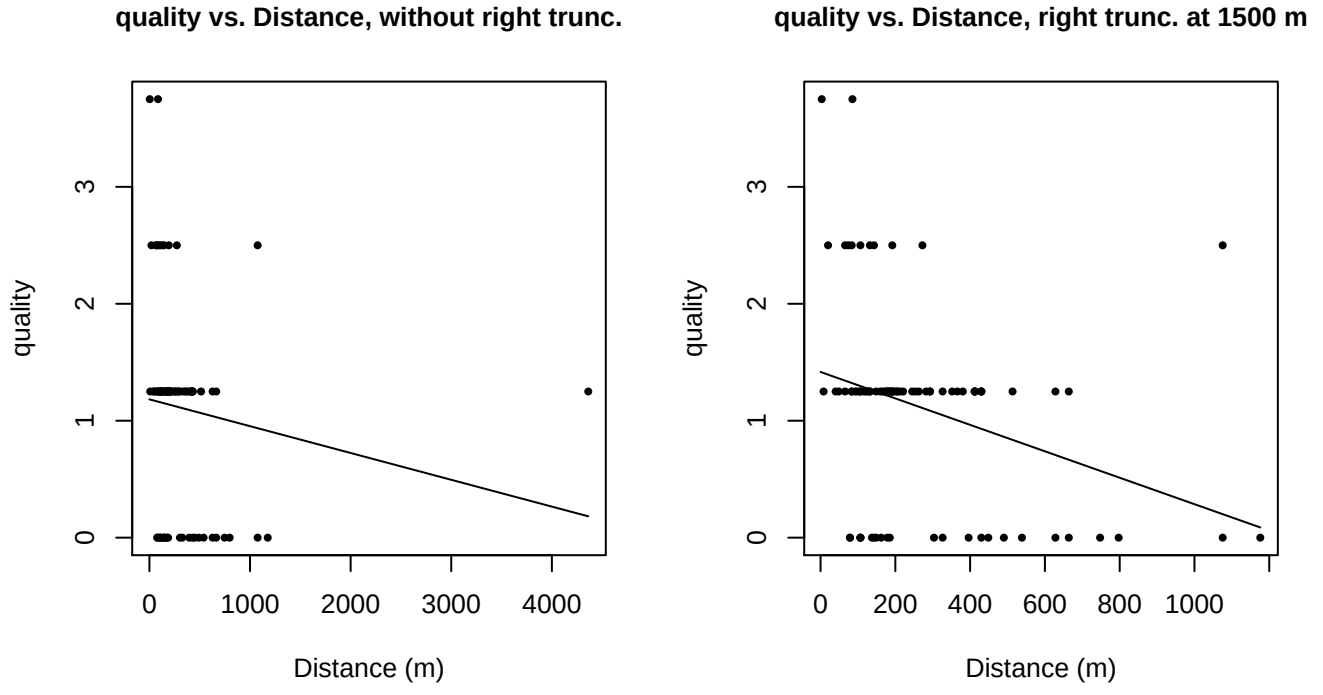

Figure 28: Scatterplots showing the relationship between the survey-specific index of the quality of observation conditions and perpendicular sighting distance, for all sightings (left) and only those not right truncated (right). Low values of the quality index correspond to better observation conditions. The line is a simple linear regression.

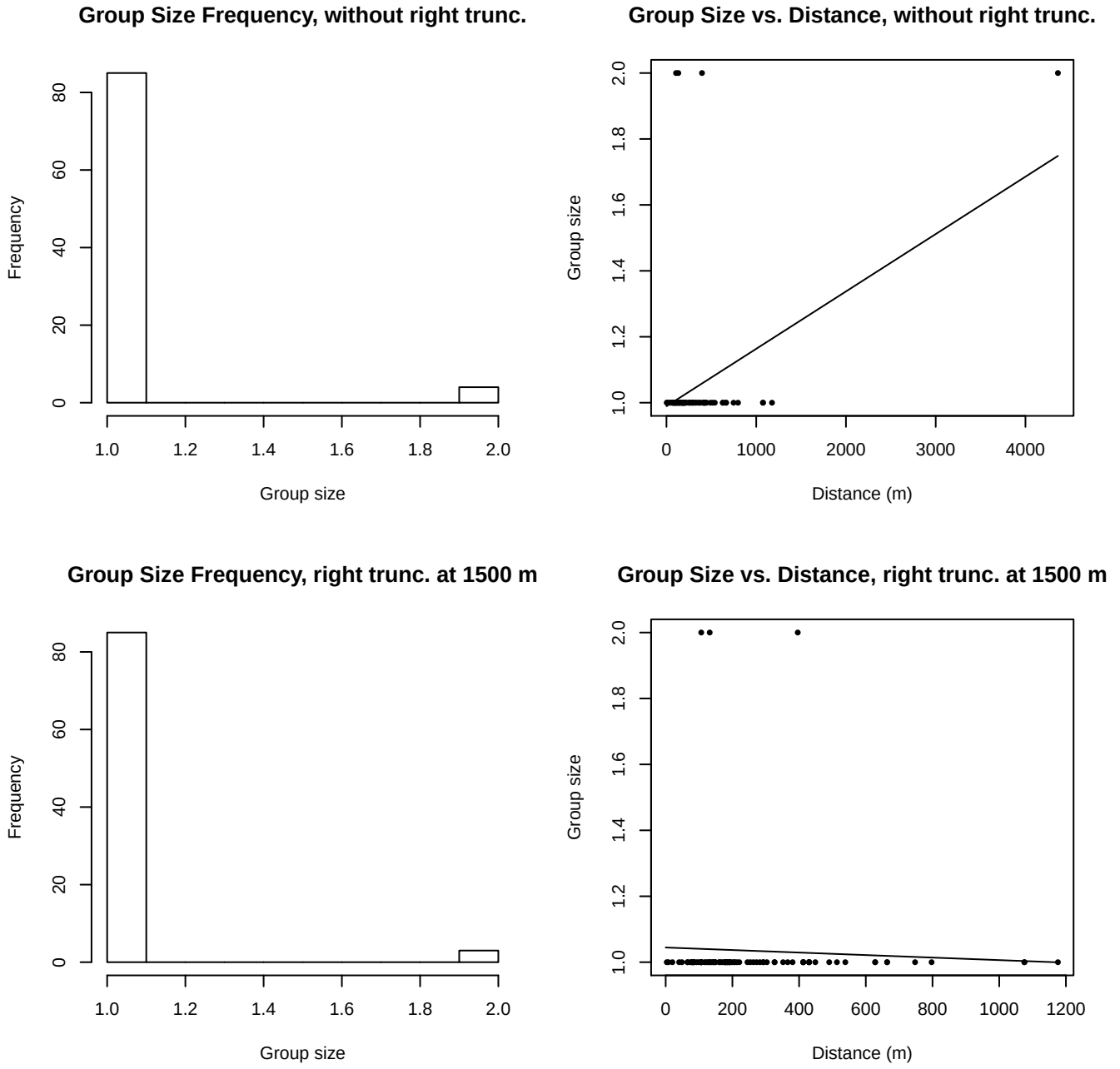

Figure 29: Histograms showing group size frequency and scatterplots showing the relationship between group size and perpendicular sighting distance, for all sightings (top row) and only those not right truncated (bottom row). In the scatterplot, the line is a simple linear regression.

NARWSS Twin Otters

Because this taxon was sighted too infrequently to fit a detection function to its sightings alone, we fit a detection function to the pooled sightings of several other species that we believed would exhibit similar detectability. These "proxy species" are listed below.

Reported By Observer	Common Name	n
Balaenoptera acutorostrata	Minke whale	731
Kogia	Pygmy or dwarf sperm whale	0

Kogia breviceps	Pygmy sperm whale	0
Kogia sima	Dwarf sperm whale	0
Mesoplodon	Beaked whale	7
Mesoplodon bidens	Sowerby's beaked whale	0
Mesoplodon densirostris	Blainville's beaked whale	0
Mesoplodon europaeus	Gervais' beaked whale	0
Mesoplodon mirus	True's beaked whale	0
Ziphiidae	Unidentified beaked whale	0
Ziphius cavirostris	Cuvier's beaked whale	0
Total		738

Table 17: Proxy species used to fit detection functions for NARWSS Twin Otters. The number of sightings, n, is before truncation.

The sightings were right truncated at 2000m. Due to a reduced frequency of sightings close to the trackline that plausibly resulted from the behavior of the observers and/or the configuration of the survey platform, the sightings were left truncted as well. Sightings closer than 107 m to the trackline were omitted from the analysis, and it was assumed that the the area closer to the trackline than this was not surveyed. This distance was estimated by inspecting histograms of perpendicular sighting distances. The vertical sighting angles were heaped at 10 degree increments up to 80 degrees and 1 degree increments thereafter, so the candidate detection functions were fitted using linear bins scaled accordingly.

Covariate	Description
beaufort	Beaufort sea state.
quality	Survey-specific index of the quality of observation conditions, utilizing relevant factors other than Beaufort sea state (see methods).
size	Estimated size (number of individuals) of the sighted group.

Table 18: Covariates tested in candidate "multi-covariate distance sampling" (MCDS) detection functions.

Key	Adjustment	Order	Covariates	Succeeded	Δ AIC	Mean ESHW (m)
hn	cos	2		Yes	0.00	599
hr				Yes	2.33	683
hr			beaufort	Yes	3.87	686
hr			quality	Yes	3.94	677
hr	poly	2		Yes	3.97	660
hr			size	Yes	4.05	684
hr	poly	4		Yes	4.34	683
hr			beaufort, quality	Yes	5.55	681
hr			beaufort, size	Yes	5.55	687
hr			quality, size	Yes	5.68	677
hr			beaufort, quality, size	Yes	7.25	682
hn	cos	3		Yes	27.27	670

hn				Yes	29.27	773
hn	herm	4		Yes	30.17	770
hn			beaufort	Yes	30.57	772
hn			size	Yes	31.04	773
hn			quality	Yes	31.24	772
hn			beaufort, size	Yes	32.39	772
hn			quality, size	Yes	33.02	773
hn	cos	1		No		
hn			beaufort, quality	No		
hn			beaufort, quality, size	No		

Table 19: Candidate detection functions for NARWSS Twin Otters. The first one listed was selected for the density model.

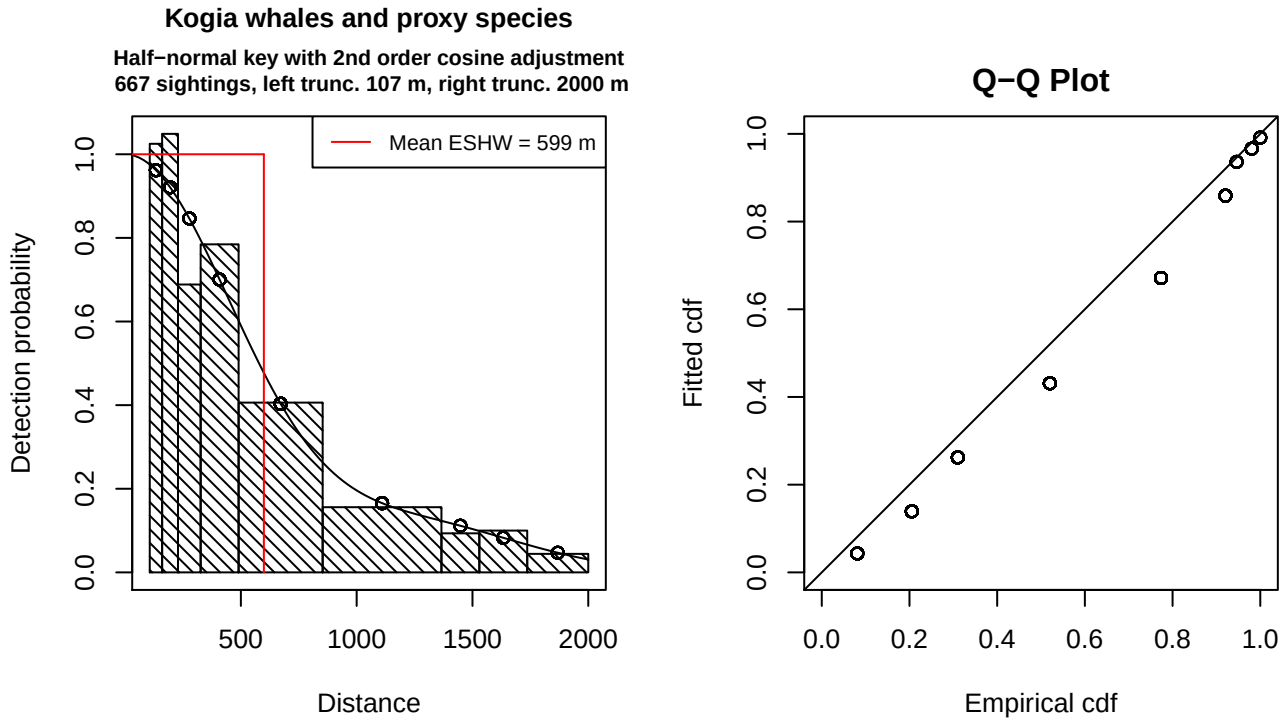

Figure 30: Detection function for NARWSS Twin Otters that was selected for the density model

Statistical output for this detection function:

```
Summary for ds object
Number of observations :  667
Distance range         :  106.5979  -  2000
AIC                    :  2606.934

Detection function:
 Half-normal key function with cosine adjustment term of order 2
```

```
Detection function parameters
Scale Coefficients:
            estimate         se
(Intercept) 6.630947 0.03193451

Adjustment term parameter(s):
              estimate         se
cos, order 2 0.3626808 0.06055252


Monotonicity constraints were enforced.
                         Estimate           SE         CV
Average p               0.2996381   0.01430097 0.04772749
N in covered region 2226.0186438 128.41505955 0.05768822

Monotonicity constraints were enforced.
```

Additional diagnostic plots:

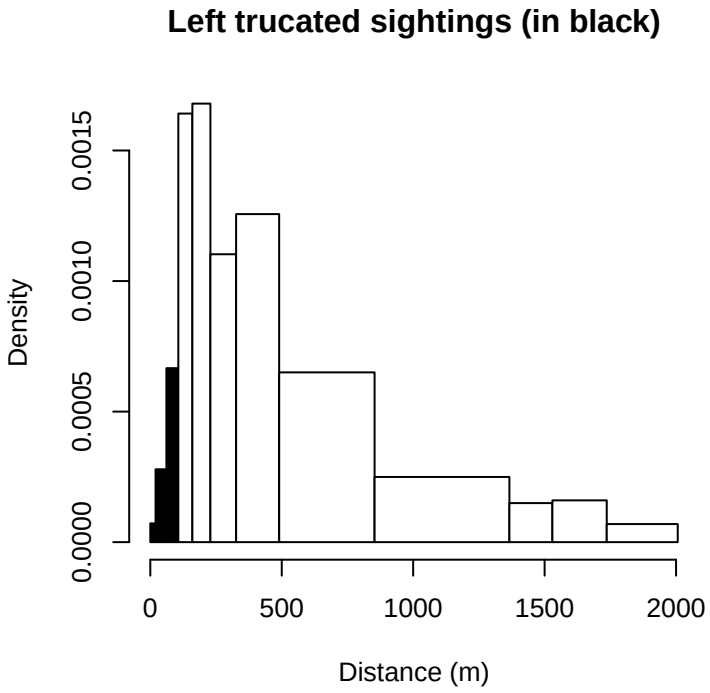

Figure 31: Density of sightings by perpendicular distance for NARWSS Twin Otters. Black bars on the left show sightings that were left truncated.

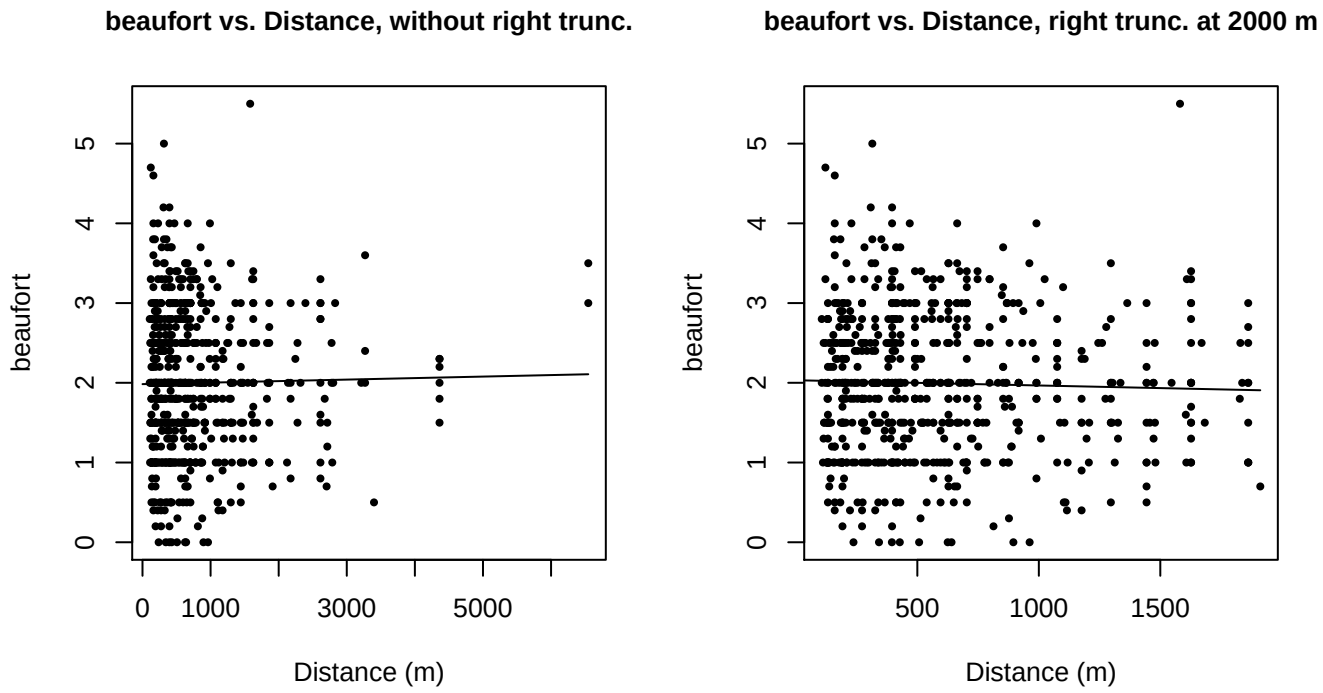

Figure 32: Scatterplots showing the relationship between Beaufort sea state and perpendicular sighting distance, for all sightings (left) and only those not right truncated (right). The line is a simple linear regression.

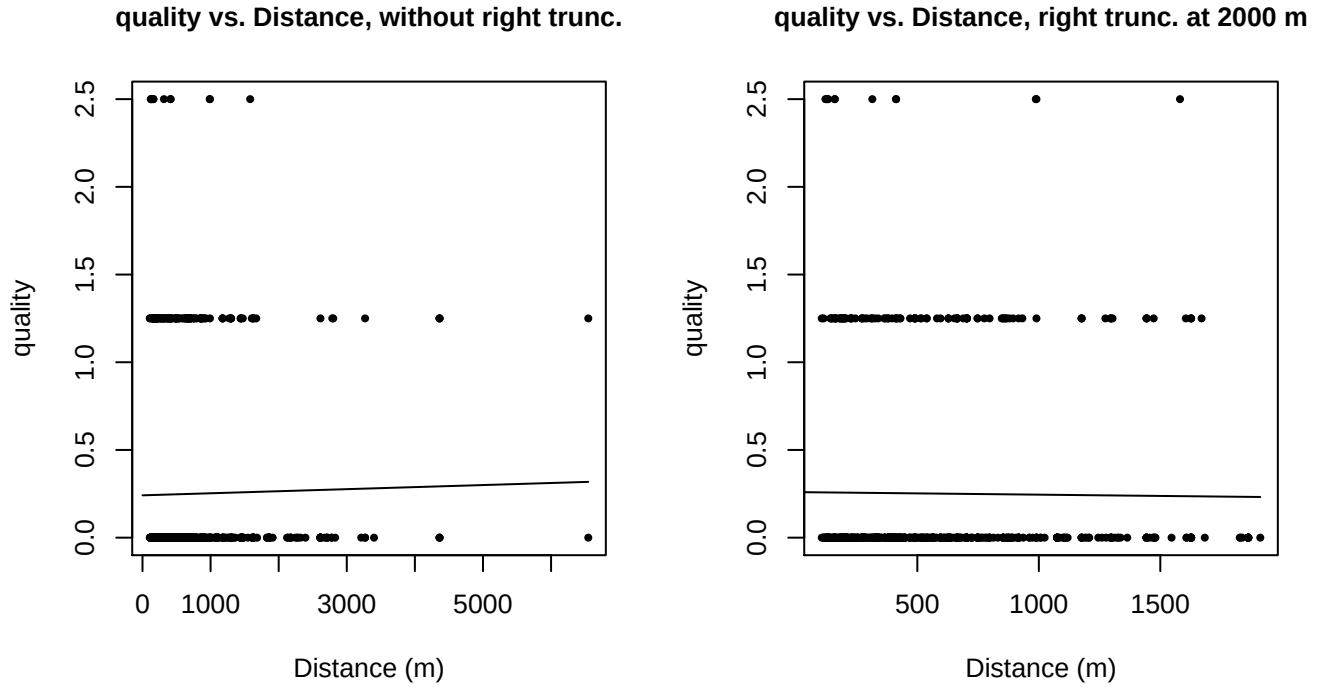

Figure 33: Scatterplots showing the relationship between the survey-specific index of the quality of observation conditions and perpendicular sighting distance, for all sightings (left) and only those not right truncated (right). Low values of the quality index correspond to better observation conditions. The line is a simple linear regression.

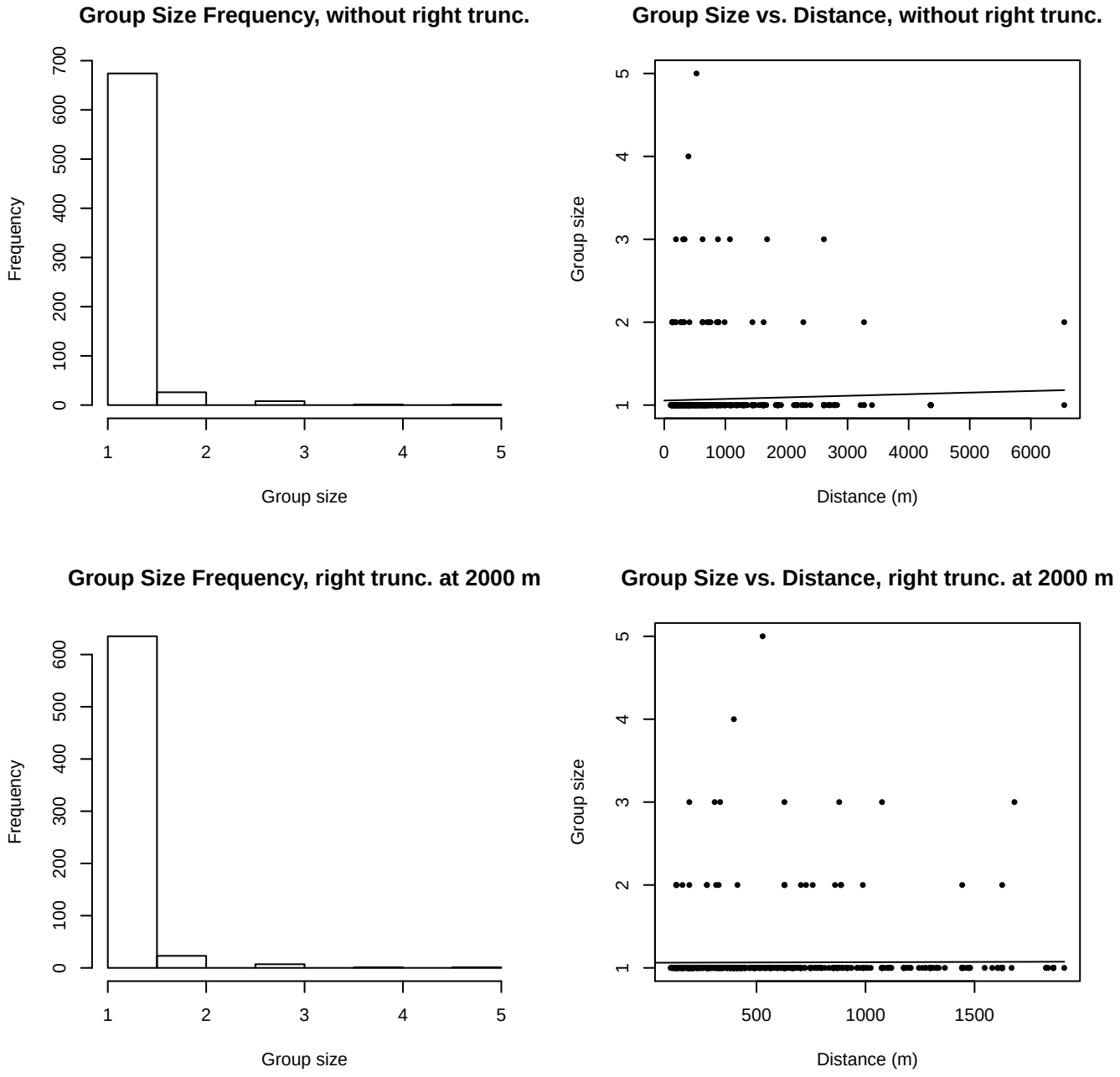

Figure 34: Histograms showing group size frequency and scatterplots showing the relationship between group size and perpendicular sighting distance, for all sightings (top row) and only those not right truncated (bottom row). In the scatterplot, the line is a simple linear regression.

g(0) Estimates

Platform	Surveys	Group Size	*g(0)*	Biases Addressed	Source
Shipboard	All	Any	0.35	Both	Barlow (1999)
Shipboard	NEFSC Abel-J Binocular Surveys	Any	0.46	Perception	Palka (2006)
Shipboard	NEFSC Endeavor	Any	0.29	Perception	Palka (2006)
Aerial	All	Any	0.12	Availability	Barlow (1999)

Table 20: Estimates of *g(0)* used in this density model.

Palka (2006) provided survey-specific g(0) estimates for two NOAA NEFSC shipboard surveys that used bigeye binoculars: the Abel-J 1998 survey (0.46) and the Endeavor 2004 survey (0.29). We used the estimates for the lower team, which was the primary team and the one for which we had sightings. These estimates used a dual-team methodology that accounted for perception bias but not availability bias.

No survey-specific g(0) estimates were available for our other shipboard surveys. For these, we relied on Barlow (1999), who estimated g(0)=0.35 using a simulation model for Kogia observed from bigeye binocular surveys that used a protocol very similar to that used by our binocular surveys. The simulation was parameterized with dive data and records of observer behavior, and accounted for both availability and perception bias. Although Barlow cautioned that his results cannot be extrapolated to other survey methods, we utilized his g(0) estimate on naked eye shipboard surveys as well, as no alternative estimate was available in the literature. But this decision turned out to be unimportant because no Kogia were sighted on any of the naked eye surveys, and thus the choice of g(0) for those surveys did not matter.

No estimate of g(0) was available in the literature for Kogia sighted on aerial surveys. Kogia are long-diving animals (Barlow, 1999), thus availability bias is likely to be substantial. Utilizing equation (3) of Carretta et al. (2000) (which follows Barlow et al. 1988), we computed the availability bias component of g(0) from the median duration of surfacing series and long dives (78 s and 10.9 min) for Kogia spp. near California reported by Barlow (1999). We did not incorporate an estimate of perception bias, thus our g(0) estimate is likely to be biased high.

Density Model

The two extant species of Kogia, the dwarf sperm whale (Kogia sima) and the pygmy sperm whale (Kogia breviceps), are very difficult for observers to distinguish at sea (Jefferson and Schiro 1997). Both species occur worldwide in tropical to temperate seas, generally in oceanic waters (Waring et al. 2013; Bloodworth and Odell 2008; Willis and Baird 1998). Although pygmy sperm whales are considered a more temperate species, the habitats and diets of the two species overlap substantially; they are often found over the continental slope, possibly to feed on cephalopods, a staple of their diet (Bloodworth and Odell 2008).

The large majority of sightings reported by the surveys included in our study reported "dwarf or pygmy sperm whale" as the taxonomic identification, and too few fully-identified sightings were reported to fit a habiat-based model for classifying the ambiguous ones. But given the apparent overlap in their habitats, we are uncertain that such an approach would be successful anyway. In any case, we modeled both species as a guild, as NOAA as historically done (Mullin and Fulling 2003; Palka 2006).

In the east coast study area, all sightings reported over the study period (1992-2014) occurred off the continental shelf. We found no definitive descriptions in the literature of seasonal movements by Kogia in this area. Accordingly, we fitted a year-round model to off-shelf waters, defined here as those deeper than the 125m isobath. With 31 sightings, we were right at the threshold we used to determine whether to fit a spatial model from environmental predictors or a stratified model that estimated mean density over the occupied area. We first fit univariate models, trying all appropriate offshore environmental predictors one at a time. All predictors were found to have statistically insignificant correlations with Kogia density and our automated modeling procedure dropped them all. Finding no environmental predictor with significant explanatory power, we reverted to an estimate of mean density over the off-shelf area.

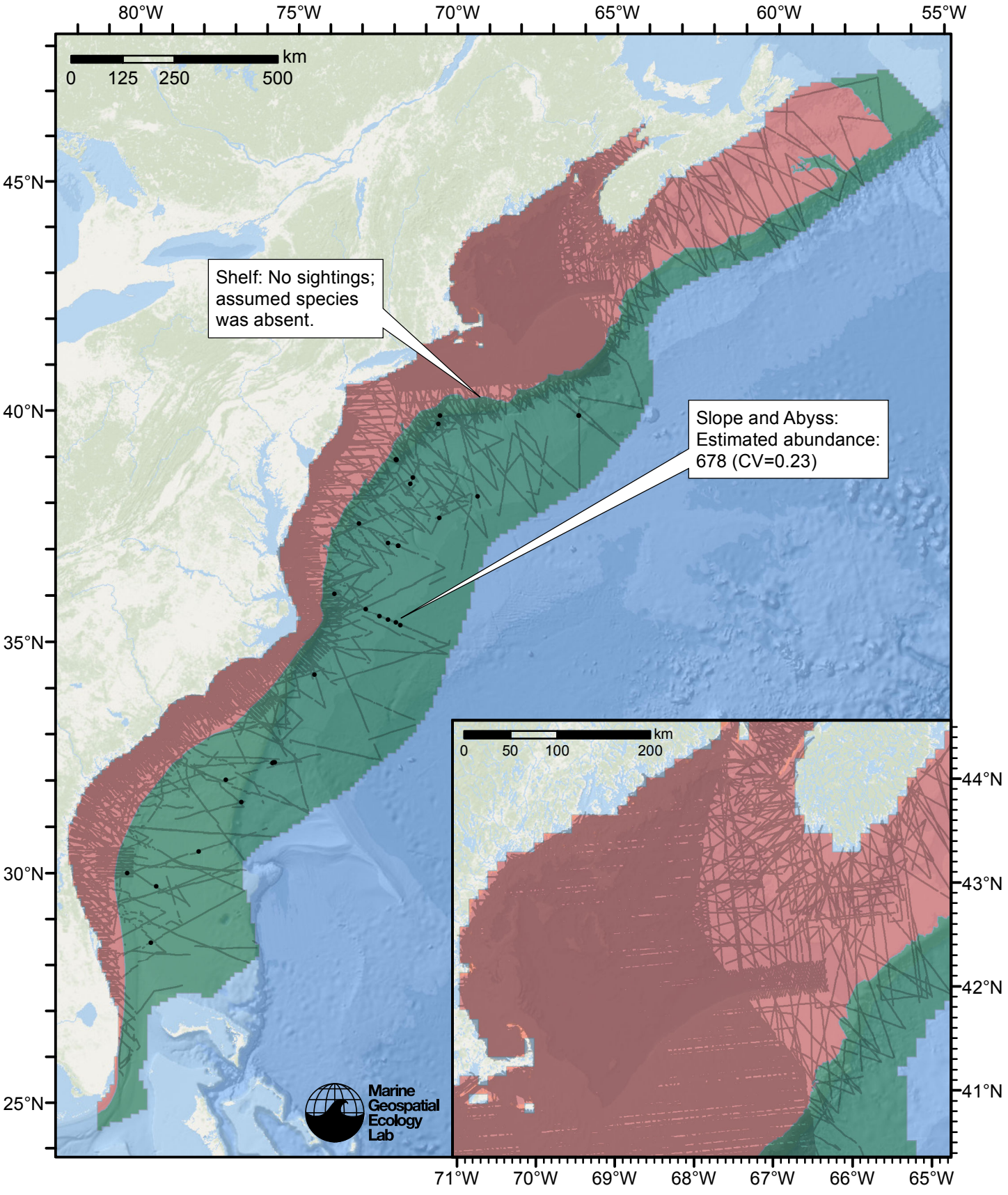

Figure 35: Kogia whales density model schematic. All sightings are shown, including those that were truncated when detection functions were fitted. The coefficient of variation (CV) underestimates the true uncertainty of our estimate, as it only incorporated the uncertainty of the GAM stage of our model. Other sources of uncertainty include the detection functions and g(0) estimates. It was not possible to incorporate these into our CV without undertaking a computationally-prohibitive bootstrap; we hope to attempt that in a future version of our model.

Abundance Estimates

Dates	Model or study	Estimated abundance	CV	Assumed g(0)=1	In our models
1992-2013	Our model	678	0.23	No	
Jun-Aug 2011	Central Virginia to lower Bay of Fundy (Waring et al. 2014)	1783	0.62	No	No
Jun-Aug 2011	Central Florida to central Virginia (Waring et al. 2014)	2002	0.69	No	No
Jun-Aug 2011	Central Florida to lower Bay of Fundy, combined	3785	0.47	No	No
Jun-Aug 2004	Maryland to Bay of Fundy (Waring et al. 2007)	358	0.44	No	Yes
Jun-Aug 2004	Florida to Maryland (Waring et al. 2007)	37	0.75	No	Yes
Jun-Aug 2004	Florida to Bay of Fundy, combined	395	0.40	No	Yes
Jul-Sep 1998	Maryland to Bay of Fundy (Waring et al. 2004)	115	0.61	No	Yes
Jul-Sep 1998	Florida to Maryland (Waring et al. 2004; Mullin and Fulling 2003)	580	0.57	Yes	Yes
Jul-Sep 1998	Florida to Bay of Fundy, combined	695	0.49	Yes/No	Yes

Table 21: Estimated mean abundance within the study area for our model and independent estimates from NOAA and/or the scientific literature. The Dates column gives the dates to which the estimates apply. For our model, these are the years for survey data were available. Our coefficient of variation (CV) estimates are probably too low, as they only incorporated the uncertainty of the GAM stage of our models. Other sources of uncertainty include the detection functions and g(0) estimates. It was not possible to incorporate these into our CVs without undertaking a computationally-prohibitive bootstrap; we hope to attempt that in a future version of our models. The Assumed g(0)=1 column specifies whether the abundance estimate assumed that detection was certain along the survey trackline. Studies that assumed this did not correct for availability or perception bias, and therefore underestimated abundance. The In our models column specifies whether the survey data from the study was also used in our models. If not, the study provides a completely independent estimate of abundance. Note that our abundance estimates are averaged over the whole year, while the other estimates apply to specific months or seasons. Please see the Discussion section below for our evaluation of our models compared to the other estimates.

Discussion

Our stratified density model predicted a mean abundance of 678, which was relatively similar to NOAA's historical estimates of 395 in 2004 and 695 in 1998. We note, however, that in 1998, NOAA's estimate for its southern area, 580, assumed that the probability of detecting an animal present on the survey trackline, g(0), was 1 (Mullin and Fulling 2003). Kogia are long-diving, cryptic animals that are often not unavailable or hard to be seen. Barlow (1999) estimated g(0)=0.35 for Kogia observed from shipboard surveys. Had NOAA used this g(0) estimate for their 1998 study, the abundance in the southern area would have been roughly three times larger.

NOAA's most recent estimate, from 2011, was an order of magnitude higher than all of these estimates. The 2011 surveys, not available to be utilized in our models, reported 43 Kogia sightings (NOAA 2011)–more than all of the sightings reported by the surveys utilized in our 1992-2014 study put together. This phenomenon appeared to reoccur in shipboard surveys in summer of 2013 (also not available for our models), which reported 68 sightings (NOAA 2013). At present, we can offer no explanation for this apparent increase in recent years. NOAA stock assessment reports indicate more strandings for recent years (Waring et al. 2013) than for the 2001-2003 period (Waring et al. 2007), but we are unsure whether the recent and historic strandings data are comparable. If they are, the apparent simultaneous increase in at-sea abundance and strandings suggests a growing abundance of Kogia in the study area.

At the time of this writing, NOAA's most recent abundance estimate of 3785 is what NOAA used to estimate stock-level parameters important to management, including the Minimum Population Estimate (Nmin) and the Potential Biological

Removal (PBR). Because this estimate is very high relative to the abundance we estimated, it is likely that if our results are used to estimate population-level impacts from potentially harmful human activities (i.e. "takes", as defined by the Marine Mammal Protection Act), the estimated impacts will be unrealistically low relative to NOAA's estimated stock size.

Because our model appears to underestimate present-day Kogia abundance and does not provide any information on the spatial distribution of Kogia beyond what NOAA's most recent estimate provides (because we could not model density from environmental covariates), our current recommendation is to use NOAA's abundance estimate, when estimating population-level impacts from potentially harmful human activities. To compute density from NOAA's abundance estimate, it is necessary to determine the geographic area (square kilometers) to which their estimate applies, then divide abundance by this area. To determine the appropriate geographic area, please contact Debra Palka (NOAA NEFSC) and Lance Garrison (NOAA SEFSC).

References

Barlow J (1999) Trackline detection probability for long diving whales. In: Marine Mammal Survey and Assessment Methods (Garner GW, Amstrup SC, Laake JL, Manly BFJ, McDonald LL, Robertson DG, eds.). Balkema, Rotterdam, pp. 209-221.

Barlow J, Oliver CW, Jackson TD, Taylor BL (1988) Harbor Porpoise, Phocoena phocoena, Abundance Estimation for California, Oregon, and Washington: II. Aerial Surveys. Fishery Bulletin 86: 433-444.

Bloodworth BE, Odell DK (2008) Kogia breviceps (Cetacea: Kogiidae). Mammalian Species 819: 1-12.

Carretta JV, Lowry MS, Stinchcomb CE, Lynn MS, Cosgrove RE (2000) Distribution and abundance of marine mammals at San Clemente Island and surrounding offshore waters: results from aerial and ground surveys in 1998 and 1999. Administrative Report LJ-00-02, available from Southwest Fisheries Science Center, P.O. Box 271, La Jolla, CA USA 92038. 44 p.

Jefferson TA, Schiro AJ (1997) Distribution of cetaceans in the offshore Gulf of Mexico. Mammal Rev. 27(1): 27-50.

Mullin KD, Fulling GL (2003) Abundance of cetaceans in the southern U.S. North Atlantic Ocean during summer 1998. Fish. Bull. 101: 603-613.

NOAA (2011) 2011 Annual Report to the Inter-Agency Agreement M10PG00075/0001: A Comprehensive Assessment of Marine Mammal, Marine Turtle, and Seabird Abundance and Spatial Distribution in US Waters of the western North Atlantic Ocean. Available at: http://www.nefsc.noaa.gov/psb/AMAPPS/docs/NMFS_AMAPPS_2011_annual_report_final_BOEM.pdf

NOAA (2013) 2013 Annual Report to A Comprehensive Assessment of Marine Mammal, Marine Turtle, and Seabird Abundance and Spatial Distribution in US Waters of the western North Atlantic Ocean. Available at: http://www.nefsc.noaa.gov/read/protspp/mainpage/AMAPPS/docs/NMFS_AMAPPS_2013_annual_report_FINAL3.pdf

Palka DL (2006) Summer Abundance Estimates of Cetaceans in US North Atlantic Navy Operating Areas. US Dept Commer, Northeast Fish Sci Cent Ref Doc. 06-03: 41 p.

Waring GT, Josephson E, Fairfield-Walsh CP, Maze-Foley K, eds. (2007) U.S. Atlantic and Gulf of Mexico Marine Mammal Stock Assessments – 2007. NOAA Tech Memo NMFS NE 205; 415 p.

Waring GT, Josephson E, Maze-Foley K, Rosel PE, eds. (2013) U.S. Atlantic and Gulf of Mexico Marine Mammal Stock Assessments – 2012. NOAA Tech Memo NMFS NE 223; 419 p.

Waring GT, Josephson E, Maze-Foley K, Rosel PE, eds. (2014) U.S. Atlantic and Gulf of Mexico Marine Mammal Stock Assessments – 2013. NOAA Tech Memo NMFS NE 228; 464 p.

Waring GT, Pace RM, Quintal JM, Fairfield CP, Maze-Foley K, eds. (2004) US Atlantic and Gulf of Mexico Marine Mammal Stock Assessments – 2003. NOAA Tech Memo NMFS NE 182; 287 p.

Willis PM, Baird RW (1998) Status of the dwarf sperm whale, Kogia simus, with special reference to Canada. Canadian Field-Naturalist 112: 114-125